Direct and Indirect Pathway Neurons in Ventrolateral Striatum Differentially Regulate Licking Movement and Nigral Responses

Zhaorong Chen[1,2,4], Zhi-Yu Zhang[1,2,4], Taorong Xie[1], Wen Zhang[1], Yaping Li[1], Xiao-Hong Xu[1,3] and Haishan Yao[1,3,5,*]

[1]Institute of Neuroscience, State Key Laboratory of Neuroscience, CAS Center for Excellence in Brain Science and Intelligence Technology, Chinese Academy of Sciences, Shanghai 200031, China

[2]University of Chinese Academy of Sciences, Beijing 100049, China

[3]Shanghai Center for Brain Science and Brain-Inspired Intelligence Technology, Shanghai 201210, China

[4]These authors contributed equally to this work

[5]Lead contact

[*]Correspondence: haishanyao@ion.ac.cn

SUMMARY

Drinking behavior in rodents is characterized by stereotyped, rhythmic licking movement, which is regulated by the basal ganglia. It is unclear how direct and indirect pathways control the lick bout and individual lick event. We find that inactivating D1 and D2 receptors-expressing medium spiny neurons (MSNs) in the ventrolateral striatum (VLS) oppositely alters the number of licks in a bout. D1- and D2-MSNs exhibit similar patterns of lick sequence-related activity but different phases of oscillation time-locked to the lick cycle. On timescale of a lick cycle, transient inactivation of D1-MSNs during tongue protrusion reduces lick probability, whereas transient inactivation of D2-MSNs has no effect. On timescale of a lick bout, inactivation of D1-MSNs (D2-MSNs) causes rate increase (decrease) in a subset of basal ganglia output neurons that decrease firing during licking. Our results reveal the distinct roles of D1- and D2-MSNs in regulating licking at both coarse and fine timescales.

Keywords

Ventrolateral striatum; licking; medium spiny neurons; oscillatory activity; substantia nigra pars reticulata

INTRODUCTION

The basal ganglia circuits are critical for action initiation and execution (Albin et al., 1989; DeLong, 1990; Hikosaka et al., 2000; Klaus et al., 2019; Mink, 1996; Park et al., 2020). Striatal medium spiny neurons (MSNs) in the input nucleus of the basal ganglia are divided to two classes according to their projection patterns (Gerfen et al., 1990; Gong et al., 2007; Smith et al., 1998). The direct pathway striatal MSNs express the D1-type dopamine receptors (D1-MSNs) and project directly to the substantia nigra pars reticulata (SNr) and internal globus pallidus (GPi), the output nuclei of basal ganglia. The indirect pathway striatal MSNs express the D2-type dopamine receptors (D2-MSNs) and project indirectly to the output nuclei via the external globus pallidus and the subthalamic nucleus. According to the classical rate model, the direct and indirect pathways facilitate and inhibit movement, respectively (Albin et al., 1989; DeLong, 1990). Optogenetic activation of D1-MSNs increases movement, whereas activation of D2-MSNs decreases movement (Kravitz et al., 2010; Oldenburg and Sabatini, 2015; Tecuapetla et al., 2014), consistent with the rate model. However, cell-type specific recordings found that both D1- and D2-MSNs are activated during voluntary movement, and the concurrent activation model proposes that the direct pathway activity supports the desired movement and the indirect pathway activity inhibits the competing movements (Barbera et al., 2016; Cui et al., 2013; Isomura et al., 2013; Jin et al., 2014; London et al., 2018; Meng et al., 2018; Tecuapetla et al., 2014). Neurons in the direct and indirect pathways are also found to differ in relative timing at sub-second timescales (Markowitz et al., 2018; O'Hare et al., 2016; Sippy et al., 2015)

and during different moments of action sequence (Geddes et al., 2018; Jin et al., 2014). It is suggested that the precise activity patterns in both pathways are required for appropriate action sequence (Geddes et al., 2018; Tecuapetla et al., 2016). However, the temporally precise relationship between activity in direct and indirect pathways is not well understood, and the functional role of D1- and D2-MSNs activity at sub-second timescale remains to be investigated.

The outputs of striatal D1- and D2-MSNs converge in the SNr and GPi, whose activity exerts inhibitory influence on neurons in thalamocortical and brainstem motor circuits (DeLong, 1990; Gerfen et al., 1990; Hikosaka et al., 2000; Nelson and Kreitzer, 2014; Redgrave et al., 1999; Smith et al., 1998). The classical model predicts that the direct and indirect pathways inhibit and disinhibit the responses of SNr neurons, respectively (Albin et al., 1989; DeLong, 1990). However, optogenetic activation of D1- or D2-MSNs induced heterogenous response changes in SNr, in which both inhibited and exited cells were observed (Freeze et al., 2013). Optogenetic inhibition of D1-MSNs and D2-MSNs did not result in opposing activity change in SNr neurons as predicted by the classical model (Tecuapetla et al., 2014). During movement, decrease and increase in firings were found for different SNr neurons (Fan et al., 2012; Gulley et al., 2002; Liu et al., 2020). It is unclear how the endogenous activity of D1- or D2-MSNs influences the firings of SNr neurons that exhibit different response patterns during movement execution.

Rhythmic licking behavior in rodent consists of stereotyped tongue movements at a frequency of 6–9 Hz (Rossi et al., 2016; Rossi and Yin, 2015; Weijnen, 1998). In the

basal ganglia circuit, the ventrolateral striatum (VLS) receives inputs from motor and somatosensory cortical areas of the mouth region (Hintiryan et al., 2016). Lesions of the VLS in rats impaired the movements of the tongue (Pisa, 1988; Pisa and Schranz, 1988) and disrupted the stereotyped motor pattern during prey capture using mouth (dos Santos et al., 2012; dos Santos et al., 2007). Activation of direct and indirect pathways in VLS induced and suppressed licking, respectively (Bakhurin et al., 2020; Lee et al., 2020). As both striatal and SNr neurons were found to exhibit lick-related activities (Aldridge and Berridge, 1998; Bakhurin et al., 2016; Gulley et al., 2002; Mittler et al., 1994; Rossi et al., 2016; Sales-Carbonell et al., 2018; Shin et al., 2018), it is of interest to use licking behavior to examine the temporal response patterns of D1- and D2-MSNs in VLS, and how striatal activities in the two pathways regulate the responses of SNr neurons during licking.

In this study, we used a voluntary licking task in head-fixed mice to examine the functional roles of D1- and D2-MSNs in regulating licking movement. On a fine timescale within hundreds of milliseconds, we found that D1- and D2-MSNs exhibited distinct patterns of oscillatory activity during the lick cycle, and transient inactivation of D1- but not D2-MSNs reduced lick probability. During execution of licking, inactivation of D1- and D2-MSNs led to distinct response changes in sub-populations of lick-related SNr neurons. Thus, our data support that the direct and indirect pathway striatal neurons exhibit temporally distinct activity patterns and differentially modulates basal ganglia output responses.

RESULTS

Opponent Regulation of Licking Behavior by D1- and D2-MSNs in VLS

Head-fixed mice were trained to voluntarily lick from a drinking spout (Figure 1A). The duration of an individual lick was defined as the time period the tongue contacted the spout, whereas the inter-lick interval was the interval between the onsets of two consecutive licks (Figure S1A). To encourage the mice to display clusters of licks as well as periods of no licks, the delivery of sucrose (10%) was triggered if a lick was preceded by at least 1 s of no licks (Figure S1B). A valid lick bout, which triggered the delivery of sucrose and the subsequent consumption, was defined as a group of licks in which the first lick was preceded by ≥ 1 s of no licks, the inter-lick interval of the first three licks was ≤ 0.3 s, and the last lick was followed by ≥ 0.5 s of no licks. We found that the lick duration was 40.53 ± 1.66 ms (mean ± SEM) and the inter-lick interval was 146.24 ± 1.99 ms (mean ± SEM, n = 9 mice, Figure S1C), consistent with the licking frequency of 6–9 Hz reported by previous studies (Rossi and Yin, 2015; Weijnen, 1998). When the time window of lick-triggered delivery of sucrose lasted for 4 s, the number of licks in a valid lick bout was 23 ± 1.66 (mean ± SEM), and the bout length was 3.41 ± 0.22 s (mean ± SEM, n = 9 mice, Figure S1C).

To examine the necessity of VLS activity in regulating licking action, we bilaterally injected AAV2/5-hSyn-hGtACR1-EGFP-WPRE in VLS and implanted optical fibers above the injection site (Figure 1B). In laser-on trials, 2 s of laser stimulation was triggered by the first lick of a lick bout that was preceded by ≥ 1 s of no licks (Figure S1B). For both laser-off and laser-on trials, the time window of lick-triggered delivery

of sucrose lasted for 3 s. In vivo recordings verified that laser stimulation reduced the firing rates of VLS neurons in awake mice (Figure S2A and S2B). As shown by the example mouse in Figure 1A, laser stimulation reduced the number of licks in a bout and decreased the instantaneous lick rate. Across the population of mice, optogenetic inactivation of VLS caused a significant reduction in the amplitude of lick PSTH ($F_{(1, 5)} = 10.51$, $p = 0.023$, two-way repeated measures ANOVA, Figure 1C). We also computed lick rate using licks within the first 2 s of lick bout, and found that optogenetic inactivation of VLS resulted in a significant decrease of lick rate ($p = 0.031$, $n = 6$, Wilcoxon signed rank test, Figure 1D). Inactivation of VLS reduced the number of licks per bout ($p = 0.031$, $n = 6$, Wilcoxon signed rank test), without affecting the inter-lick interval ($p = 0.44$, Wilcoxon signed rank test, Figure 1D), suggesting that VLS inactivation causes reduction in lick rate by early termination of lick bout without affecting the lick rhythm. For control mice in which AAV2/8-hSyn-eGFP-3Flag-WPRE-SV40pA was injected in VLS (Figure S1D), laser stimulation did not affect the lick PSTH ($F_{(1, 7)} = 0.097$, $p = 0.77$, two-way repeated measures ANOVA, Figure 1E).

Unlike VLS inactivation, inactivation of the dorsal striatum (DS) did not cause a significant change in the amplitude of lick PSTH ($F_{(1, 5)} = 0.11$, $p = 0.75$, two-way repeated measures ANOVA, Figure 1F and Figure S1E). Among the three groups of mice (VLS-EGFP, VLS-GtACR1 and DS-GtACR1), the reduction in lick rate and in number of licks per bout for the VLS-GtACR1 group was significantly larger than those for other groups (lick rate: $F_{(2, 17)} = 8.71$, $p = 2.48\times10^{-3}$, number of licks per bout: $F_{(2, 17)} = 16.23$, $p = 1.14\times10^{-4}$, one-way ANOVA followed by Sidak's multiple comparisons

test, $p < 0.01$, Figure 1G and 1H). Thus, these results demonstrate that the VLS but not the DS is involved in motor control of licking behavior.

To test the role of D1- and D2-MSNs in VLS in licking behavior, we bilaterally injected AAV2/8-CAG-DIO-GtACR1-P2A-EGFP in the VLS of D1-Cre or D2-Cre mice (Figure S1F and S1G). Slice recordings confirmed that laser stimulation could suppress the firing rates of D1- and D2-MSNs in VLS (Figure S2C). We found that inactivation of D1-MSNs in VLS significantly decreased the amplitude of lick PSTH ($F_{(1, 10)} = 12.82$, $p = 0.005$, two-way repeated measures ANOVA, Figure 1I), lick rate ($p = 0.0029$, Wilcoxon signed rank test) and number of licks per bout ($p = 0.0088$, $n = 11$ mice, Wilcoxon signed rank test, Figure 1J), whereas inactivation of D2-MSNs significantly increased the amplitude of lick PSTH ($F_{(1, 12)} = 36.41$, $p = 5.90\times10^{-5}$, two-way repeated measures ANOVA, Figure 1K), lick rate ($p = 2.44\times10^{-4}$, Wilcoxon signed rank test) and number of licks per bout ($p = 0.0015$, $n = 13$ mice, Wilcoxon signed rank test, Figure 1L). Inactivation of D1-MSNs or D2-MSNs did not affect the inter-lick interval ($p = 0.90$ and 0.54, respectively, Wilcoxon signed rank test, Figure 1J and 1L). Laser stimulation did not affect lick PSTH ($F_{(1, 10)} = 0.13$, $p = 0.72$, two-way repeated measures ANOVA), lick rate ($p = 0.97$, Wilcoxon signed rank test) or number of licks per bout ($p = 0.55$, $n = 11$ mice, Wilcoxon signed rank test) for control D1-Cre or D2-Cre mice in which AAV2/8-hSyn-FLEX-tdTomato was injected in the VLS (Figure S1H–S1J and Figure S2D). Thus, the results demonstrate that the activity of D1- and D2-MSNs in VLS oppositely regulates licking action, consistent with a previous report (Bakhurin et al., 2020).

D1- and D2-MSNs Exhibit Similar Lick-sequence Related Activity

To examine the activity patterns of D1- and D2-MSNs in VLS, we performed electrophysiological recordings using optrode from D1-Cre or D2-Cre mice in which AAV2/8-Syn-FLEX-ChrimsonR-tdTomato were injected in VLS (Figure 2A, 2C and Figure S3A). A unit was identified as ChrimsonR-expressing if it satisfied the two criteria (Lee et al., 2019): 1) significantly responded to laser stimulation with a spike latency < 6 ms, and 2) the Pearson's correlation coefficient between waveforms of spontaneous spikes and laser-evoked spikes was > 0.95 (Figure 2B, 2D and Figure S3B). During licking behavior, the delivery of sucrose was triggered if a lick was preceded by ≥ 1.5 s of lick suppression, and the time window of lick-triggered delivery of sucrose lasted for 3 s. Licking parameters, including inter-lick interval, number of licks per bout and bout length, were similar between D1-Cre and D2-Cre mice (Figure S3C). We classified the identified ChrimsonR-expressing units into putative MSNs and other neurons according to their spike waveforms and coefficients of variation (CV) of inter-spike intervals (Shin et al., 2018) (Figure S3D and S3E). The responses of MSNs (Figure 2E–2H) during licking behavior were analyzed.

Previous studies using lever-press task found that striatal neurons can signal the initiation, execution, and termination of learned action sequence (Jin and Costa, 2010, 2015; Jin et al., 2014; Martiros et al., 2018; Vandaele et al., 2019). We examined whether the activities of D1- and D2-MSNs in VLS are related to the execution or start/stop of licking. A trial of lick bout was defined to include a baseline phase (from -

1 to -0.5 s relative to bout onset), a start phase (from -0.5 to 0.25 s relative to bout onset), an execution phase (the duration of the lick bout), and a stop phase (from -0.25 to 0.5 s relative to bout offset). By comparing the responses between the baseline phase and the start (execution, or stop) phase, we classified a unit as start, stop, boundary, sustained, or inhibited neuron (Figure 2F, see STAR Methods). Neurons that were classified as one of these response types were considered to exhibit lick-related activities. We found that neither the percentage of lick-related neurons ($\chi^2_{(1)} = 0.23$, $p = 0.63$, Figure 2G) nor the percentage of response types differed between D1- and D2-MSNs ($\chi^2_{(4)} = 5.88$, $p = 0.21$, D1-MSNs: n = 76 lick-related neurons out of a total of 87 neurons, D2-MSNs: n = 70 lick-related neurons out of a total of 78 neurons, Figure 2H). Thus, D1- and D2-MSNs exhibited similar patterns of lick-sequence related activities during licking movement.

D1- and D2-MSNs Exhibit Different Phase Relationships with the Lick Cycle

A prominent feature of licking behavior is the rhythmic alternation of tongue protrusions and retractions (Travers et al., 1997; Weijnen, 1998). The period of a lick cycle was ~150 ms, which could be observed from the peri-event time histogram (PETH) computed using licks around ±200 ms of each lick (Figure 3A and 3B, see STAR Methods) (Rossi et al., 2016). We next examined whether MSNs in VLS show oscillatory activity related to the lick cycle (Rossi et al., 2016). We calculated lick-triggered spike PETH using spikes occurring around ±200 ms of each lick (Figure 3A and 3B), and then computed the Pearson's correlation coefficient between the lick

PETH and the lick-triggered spike PETH (Figure 3C and 3D) or between the lick PETH and the lick-triggered spike PETH shifted by 40 ms (corresponding to a phase shift of ~90°) (Figure S4, see STAR Methods). For those neurons in which the correlation coefficient was significant, the lick-triggered spike PETHs clearly showed oscillatory activity (Figure 3A, 3B and Figure S4). To determine the oscillatory phase relative to the lick cycle (-180° to 180°), we identified the time at which the amplitude of lick-triggered spike PETH was maximum and transformed it to polar coordinate. The phase of peak response was significantly different between D1- and D2-MSNs ($p = 5.49\times10^{-4}$, n = 66 and 58 for D1-MSNs and D2-MSNs, respectively, circular Watson-Williams two-sample test (Berens, 2009), Figure 3E and 3F). When we averaged the z-scored lick-triggered spike PETHs across units, we found significant difference between the oscillatory activities of D1- and D2-MSNs ($F_{interaction(35, 4270)} = 7.76$, $p < 1\times10^{-15}$, two-way ANOVA with mixed design, Figure 3G). While the population of D1-MSNs showed a peak response around 0°, corresponding to the time of tongue contact with the lick spout, the peak of population D2-MSNs was around 90°, which was near the time of tongue retraction from the lick spout. These data suggest that the activity of D1- and D2-MSNs exhibits distinct phase relationships with the lick cycle.

Transient Inactivation of D1-MSNs during Tongue Protrusion Reduces Lick Probability

We wondered whether transient perturbation of D1- or D2-MSNs activity at a timescale within the lick cycle affects individual lick event. We bilaterally injected

AAV2/8-CAG-DIO-GtACR1-P2A-EGFP in the VLS of D1-Cre or D2-Cre mice, which were then trained to perform voluntary licking behavior. As the peak of lick-triggered oscillatory activity in population D1-MSNs was around 0°, we applied transient laser stimulation (duration = 25 ms) around the time of tongue protrusion. After the initiation of a lick bout, laser stimulation was triggered after an inter-lick interval following the onset of the second lick (Figure 4A and 4B, see STAR Methods). For the population of D1-Cre mice tested, transient inactivation of D1-MSNs significantly reduced the amplitude of lick signal for the third lick event ($F_{(1, 6)} = 78.2$, $p = 1.16\times10^{-4}$, two-way repeated measures ANOVA, Figure 4B) and the probability of the third lick ($p = 0.016$, Wilcoxon signed rank test), without affecting the probability of the fourth lick ($p = 0.58$, Wilcoxon signed rank test, Figure 4C) or the length of lick bout ($p = 0.58$, $n = 7$ mice, Wilcoxon signed rank test, Figure 4D). Unlike perturbation of D1-MSNs, transient inactivation of D2-MSNs in VLS around the time of tongue protrusion did not change the lick signal ($F_{(1, 5)} = 1.2$, $p = 0.32$, two-way repeated measures ANOVA), the probability of the third lick ($p = 0.69$, Wilcoxon signed rank test) or the length of lick bout ($p = 1$, $n = 6$ mice, Wilcoxon signed rank test, Figure 4E–4H). Inactivation of D2-MSNs for 150 ms at a later time (3 s after bout onset), when lick rate was lower, still did not affect licking behavior (Figure S5A). For control D1-Cre mice in which AAV2/8-hSyn-FLEX-tdTomato was injected in VLS, the amplitude of lick signal, the lick probability or the bout length was not affected by transient laser stimulation (Figure S5B–S5D). Thus, the activity of D1-MSNs in VLS around tongue protrusion, which is in the range of tens of millisecond, is necessary for the execution of individual lick

event.

Differential Roles of Endogenous D1- and D2-MSNs Activity in Controlling SNr Responses during Licking Movement

By injecting CTB in VLS, we observed anterogradely labelled fibers in the lateral SNr (Figure S6A), consistent with previous reports (Lee et al., 2020; von Krosigk et al., 1992). To examine how the endogenous activity of D1- or D2-MSNs influences the downstream neurons, we bilaterally injected AAV2/8-CAG-DIO-GtACR1-P2A-EGFP in VLS of D1-Cre or D2-Cre mice. During licking behavior, the delivery of sucrose was triggered if a lick was preceded by ≥1 s of no licks, and the time window of lick-triggered delivery of sucrose lasted for 3 s. We performed extracellular recordings from the lateral SNr of behaving mice, with and without laser stimulation in VLS (Figure 5A and 5B, Figure 6A and 6B). The units were classified as GABAergic and non-GABAergic neurons based on their spike waveforms (Figure S6B, see STAR Methods), and GABAergic SNr neurons were used for subsequent analysis.

For D1-Cre mice, we performed two sets of experiments. In the first set of experiment, 2 s of laser stimulation was triggered by the first lick of a bout (Figure 5B–5E). Inactivation of D1-MSNs in VLS caused a significant increase in the amplitude of lick PSTH ($F_{(1, 18)} = 44.46$, $p = 2.96\times10^{-6}$, two-way repeated measures ANOVA, Figure 5B), and both increase and decrease in firing rates of SNr neurons could be observed (Figure S6C). At the population level, inactivation of D1-MSNs significantly increased the firing rates in 8.13% (13/160) of SNr neurons, most of which

were classified as inhibited neurons in laser-off condition (Figure 5C), and significantly decreased the firing rates in 25% (40/160) of SNr neurons, which were predominantly sustained neurons (Figure 5D). For a large fraction of SNr neurons (66.87%, 107/160), the firing rates were not significantly affected by inactivation of D1-MSNs (Figure 5E). In the second set of experiment, 25 ms of laser stimulation was applied around the time of tongue protrusion for the third lick in a lick bout, leading to a significant decrease in the lick signal amplitude of the third lick event ($F_{(1, 11)} = 40.8$, $p = 5.2\times10^{-5}$, two-way repeated measures ANOVA, Figure 5F). When we analyzed responses within the time window of the third lick event, we found firing rate increase in 16.96% (19/112) of SNr neurons, which were predominantly inhibited neurons (Figure 5G), and firing rate decrease in 12.5% (14/112) of SNr neurons, most of which were sustained neurons (Figure 5H). Similar to the effect of 2-s laser stimulation, the responses of most SNr neurons (70.54%, 79/112) were not significantly affected by transient inactivation of D1-MSNs (Figure 5I). Thus, on both timescales of second and tens of millisecond, inactivation of D1-MSNs in VLS resulted in rate increase (decrease) for a subset of SNr neurons that showed inhibited (sustained) responses during licking.

For D2-Cre mice, we examined the effect of 2-s laser stimulation in VLS, which significantly increased the amplitude of lick PSTH ($F_{(1, 16)} = 69.26$, $p = 3.31\times10^{-7}$, two-way repeated measures ANOVA, Figure 6B), on the responses of SNr neurons (Figure S6D). In contrast to that observed in D1-Cre mice, inactivation of D2-MSNs in VLS significantly decreased the firing rates in 7.77% (8/103) of SNr neurons that were mostly of the inhibited response type (Figure 6C), and significantly increased the firing

rates in 21.36% (22/103) of SNr neurons that were predominantly sustained neurons (Figure 6D). Firing rates in 70.87% (73/103) of SNr neurons were not affected by inactivation of D2-MSNs in VLS (Figure 6E).

Thus, our results demonstrated that the endogenous activity of D1- and D2-MSNs in the striatum oppositely regulates the responses of a subset of SNr neurons during movement.

DISCUSSION

Using voluntary licking behavior in mice, we found that D1- and D2-MSNs in VLS played distinct roles in regulating licking movement. Optogenetic tagging showed that D1- and D2-MSNs exhibited similar patterns of lick sequence-related activity. At a fine timescale, however, they differed in the oscillatory activity time-locked to the lick cycle, with a large fraction of D1-MSNs showing peak response around the time of spout contact. Transient inactivation of D1-MSNs around the time of tongue protrusion reduced the lick probability, whereas transient inactivation of D2-MSNs did not affect licking. Inhibiting endogenous activity of D1- and D2-MSNs in the VLS produced opposing effects in a subset of SNr neurons that were inhibited during licking, as well as those with sustained activity during licking. These findings reveal the differential functions of direct and indirect pathway striatal neurons at fine as well as coarse timescales, and support the notion that the two pathways have opponent roles in regulating the basal ganglia output responses during movement.

Orofacial behaviors, such as sniffing, whisking, chewing and licking, are important

for sensory exploration and nutrient ingestion (Moore et al., 2014; Travers et al., 1997). Neurons in the striatum are topographically organized (Hintiryan et al., 2016; Hunnicutt et al., 2016; Liu et al., 2020), and the projections from sensorimotor cortical areas representing the mouth region terminate in VLS (Hintiryan et al., 2016). We found that optogenetic inactivation of the VLS, but not the DS, disrupted licking behavior by reducing the number of licks in a bout. This is consistent with previous reports that lesion of VLS impaired the movement of the tongue (Pisa, 1988; Pisa and Schranz, 1988), and that stimulation of VLS but not dorsomedial striatum modulated licking (Lee et al., 2020). We showed that inactivation of D1-MSNs and D2-MSNs in the VLS suppressed and increased licking, respectively, consistent with a recent work studying the effect of activating direct and indirect pathways in the VLS (Bakhurin et al., 2020).

In contrast to the opposite roles of direct and indirect pathways observed at behavioral level (Kravitz et al., 2010), cell-type-specific recordings showed that D1- and D2-MSNs are both activated during initiation and execution of voluntary movement (Barbera et al., 2016; Cui et al., 2013; Isomura et al., 2013; Jin et al., 2014; London et al., 2018; Meng et al., 2018; Parker et al., 2018; Tecuapetla et al., 2014). These findings are consistent with the proposal that the activity of direct pathway facilitates the desired movement and the coactivated indirect pathway inhibits the competing movements (Hikosaka et al., 2000; Jin et al., 2014; Klaus et al., 2019; Mink, 1996). The direct and indirect pathways are also found to exhibit different activity patterns. For instance, in mice performing learned action sequences of lever pressing, more D1-MSNs displayed sequence-related sustained activity, whereas more D2-

MSNs showed sequence-related inhibited activity (Jin et al., 2014). Whether the activity of D1- and D2-MSNs was coactive or opponent also depended on the moment in sequence execution (Geddes et al., 2018). In addition, D1- and D2-MSNs differed in response timing at sub-second timescale during whisker sensorimotor task or showed decorrelated activity in specific epochs of naturalistic behaviors (Markowitz et al., 2018; Sippy et al., 2015). Ex vivo analysis after behavioral training showed that the relative timing between D1- and D2-MSNs switched during transition from goal-directed to habitual behavior (O'Hare et al., 2016). In our study, we found that D1- and D2-MSNs in the VLS both exhibited lick sequence-related activities, with similar proportions of neurons for each response type. Interestingly, on the timescale of a lick cycle (~ 150 ms), D1- and D2-MSNs differed in the phase of lick-related oscillatory activity. The oscillatory activity averaged over population D1-MSNs peaked around the time of tongue-spout contact, whereas that for population D2-MSNs was shifted toward the time around tongue retraction. The difference between D1- and D2-MSNs activity at timescale of tens of milliseconds provides evidence for the race model, in which the coactive direct and indirect pathways neurons show different temporal profiles during movement (Klaus et al., 2019; O'Hare et al., 2016; Schmidt et al., 2013).

A previous study found that striatal activity in the direct and indirect pathways was decorrelated at fine timescales, and that the accuracy of decoding behavioral syllable identity was improved when using activity in both pathways as compared to that using activity in each pathway, suggesting that decorrelation between the two pathways is important for representing individual behavioral syllables (Markowitz et al., 2018). In

our study, we directly tested the role of fine timescale activity of D1- and D2-MSNs in licking behavior. Intriguingly, we found that transient inactivation of D1-MSNs in VLS around the time of tongue protrusion reduced the lick probability of current lick event. This demonstrates that the temporally precise activity of D1-MSNs in VLS around tongue protrusion plays a crucial role in controlling individual lick event. As the impairment of a lick event did not affect lick probability of the next lick event, our result also suggests that the innate and stereotyped licking sequence is organized in a hierarchical structure, similar to that found for learned action sequence (Geddes et al., 2018). Furthermore, while inactivation of D2-MSNs for 2 s caused an increase in lick rate, transient inactivation of D2-MSNs around the onset of the third lick event or after 3 s following bout onset did not affect licking. This suggests that, compared with the suppression of D1-MSNs activity, it may require a longer duration to inactivate D2-MSNs to drive behavioral effect. It is also of interest for future study to examine how the precise activity patterns of D1- and D2-MSNs control other rhythmic orofacial behaviors, such as sniffing and whisking.

Previous studies showed that activating the GABAergic projection from lateral SNr to superior colliculus suppressed self-initiated licking (Rossi et al., 2016; Toda et al., 2017). Consistent with these reports, we found that inactivation of VLS, which topographically projects to lateral SNr (Lee et al., 2020; von Krosigk et al., 1992), disrupted licking. The GABAergic SNr neurons provide tonic inhibition to downstream areas at the brainstem and thalamus (Hikosaka, 2007). The classical model proposed that the direct and indirect pathways facilitate and decrease movement, respectively, by

inhibiting and disinhibiting the responses of SNr neurons (DeLong, 1990; Kravitz et al., 2012). Nevertheless, optogenetic activation of striatal neurons in the direct or indirect pathway caused both decrease and increase in firing rates of SNr neurons (Freeze et al., 2013). Optogenetic inactivation of striatal neurons in the direct or indirect pathway showed that only a small fraction of SNr neurons changed activity, in which both increase and decrease was observed (Tecuapetla et al., 2014). In our study, we found that inactivation of D1- or D2-MSNs did not change the firing rates of a large fraction of SNr neurons in behaving mice. Interestingly, however, inactivation of the direct pathway striatal neurons led to rate increase for a subset of SNr neurons, most of which were inhibited during licking, and rate decrease for another subset, the majority of which showed sustained activity during licking. Inactivation of the indirect pathway striatal neurons also resulted in rate increase and rate decrease for two subsets of SNr neurons, but whose response types were predominantly sustained neurons and inhibited neurons, respectively. The paradoxical observation that inactivation of D1-MSNs (or D2-MSNs) could decrease (or increase) the firing rates of a subpopulation of SNr neurons may be due to several possibilities, including the axon collaterals of D1-MSNs in GPe (Gerfen et al., 1990; Xiao et al., 2020), the recurrent collateral connections between D2- and D1-MSNs in the striatum (Taverna et al., 2008), and that sustained neurons (or start neurons) in SNr could inhibit other sustained neurons via axon collaterals within SNr (Brown et al., 2014; Deniau et al., 1982; Deniau et al., 2007). Overall, our results are in line with the proposal that the inhibited neurons in SNr disinhibit the desired movement, whereas the sustained neurons suppress competing

movements (Cui et al., 2013; Hikosaka et al., 2000; Mink, 1996). Our results also suggest that the coactivated direct and indirect pathways striatal neurons oppositely control movement by differential regulation of SNr activity.

FIGURE LEGENDS

Figure 1. Opponent Regulation of Licking Behavior by D1- and D2-MSNs in VLS

(A) Lick rasters and lick PSTHs (200 ms/bin) for laser-off (left) and laser-on (right) trials of an example mouse, in which AAV-GtACR1 was bilaterally injected in VLS. Gray shading indicates the duration of laser stimulation.

(B) Representative fluorescence image showing the expression of AAV2/5-hSyn-hGtACR1-EGFP-WPRE in VLS of a C57BL/6 mouse.

(C) Inactivation of VLS significantly decreased the amplitude of lick PSTH ($F_{(1, 5)}$ = 10.51, p = 0.023, two-way repeated measures ANOVA). Data represent mean ± SEM. Gray shading indicates the duration of laser stimulation.

(D) Inactivation of VLS significantly reduced lick rate (p = 0.031) and number of licks per bout (p = 0.031), without affecting inter-lick interval (p = 0.44, n = 6 mice, Wilcoxon signed rank test).

(E) Laser stimulation did not significantly change the lick PSTH in control mice, in which AAV-EGFP was bilaterally injected in VLS ($F_{(1, 7)}$ = 0.097, p = 0.77, two-way repeated measures ANOVA). Data represent mean ± SEM. Gray shading indicates the duration of laser stimulation.

(F) Inactivation of DS did not significantly change the lick PSTH ($F_{(1, 5)}$ = 0.11, p = 0.75, two-way repeated measures ANOVA). Data represent mean ± SEM. Gray shading indicates the duration of laser stimulation.

(G) Comparison of the change in lick rate (difference in lick rate between laser-on and laser-off trials) among the three groups of mice (VLS-EGFP: n = 8 mice; VLS-

GtACR1: n = 6 mice; DS-GtACR1: n = 6 mice). ** $p < 0.01$, one-way ANOVA followed by Sidak's multiple comparisons test. Data represent mean ± SEM.

(H) Comparison of the change in number of licks per bout (difference in number of licks per bout between laser-on and laser-off trials) among the three groups of mice (VLS-EGFP: n = 8 mice; VLS-GtACR1: n = 6 mice; DS-GtACR1: n = 6 mice). *** $p < 0.001$, one-way ANOVA followed by Sidak's multiple comparisons test. Data represent mean ± SEM.

(I) Inactivation of D1-MSNs in VLS significantly decreased the amplitude of lick PSTH ($F_{(1, 10)} = 12.82$, $p = 0.005$, two-way repeated measures ANOVA). Data represent mean ± SEM. Gray shading indicates the duration of laser stimulation.

(J) Inactivation of D1-MSNs in VLS significantly decreased lick rate ($p = 0.0029$) and number of licks per bout ($p = 0.0088$), without affecting inter-lick interval ($p = 0.90$, n = 11 mice, Wilcoxon signed rank test).

(K) Inactivation of D2-MSNs in VLS significantly increased the amplitude of lick PSTH ($F_{(1, 12)} = 36.41$, $p = 5.90\times10^{-5}$, two-way repeated measures ANOVA). Data represent mean ± SEM. Gray shading indicates the duration of laser stimulation.

(L) Inactivation of D2-MSNs in VLS significantly increased lick rate ($p = 2.44\times10^{-4}$) and number of licks per bout ($p = 0.0015$), without affecting inter-lick interval ($p = 0.54$, n = 13 mice, Wilcoxon signed rank test).

See also Figure S1 and S2.

Figure 2. D1- and D2-MSNs Exhibit Similar Patterns of Lick-related Activities

(A) Fluorescence image of VLS for an example D1-Cre mouse in which AAV2/8-Syn-FLEX-ChrimsonR-tdTomato was injected in VLS.

(B) Spike rasters (left), waveforms and PSTH (right) of an identified D1-MSN. Time 0 is laser onset. Gray shading, laser stimulation.

(C) Fluorescence image of VLS for an example D2-Cre mouse in which AAV2/8-Syn-FLEX-ChrimsonR-tdTomato was injected in VLS.

(D) Spike rasters (left), waveforms and PSTH (right) of an identified D2-MSN. Time 0 is laser onset. Gray shading, laser stimulation.

(E) Lick rasters (left) and spike rasters (right), sorted by the length of lick bout, for an identified D1-MSN during licking behavior. Time 0 is bout onset. Orange line and curve: the start and end of lick bout.

(F) Spike rasters (left) and PSTHs (right) for example MSNs that were classified as start, stop, boundary, sustained, and inhibited neurons. The PSTHs were smoothed with a moving average of consecutive 5 bins. In the spike rasters, orange line and curve indicate the start and end of lick bout, respectively. In the PSTHs, the upper and lower edges of the gray shading indicate upper and lower thresholds, corresponding to 3 SD above and below the mean firing rate in baseline phase, respectively; the two vertical dashed lines denote the start and end of the execution phase.

(G) The percentages of lick-related and non-related neurons were not significantly different between D1-MSNs (n = 87) and D2-MSNs (n = 78) ($\chi^2_{(1)} = 0.23$, $p = 0.63$).

(H) The percentages of response types were not significantly different between lick-

related D1-MSNs (n = 76) and lick-related D2-MSNs (n = 70) ($\chi^2_{(4)} = 5.88$, p = 0.21).

See also Figure S3.

Figure 3. D1- and D2-MSNs Exhibit Different Phase Relationships with the Lick Cycle

(A) Upper, lick rasters and lick PETH computed using licks around ±200 ms of each lick for an example D1-Cre mouse. Lower, rasters and PETH of lick-triggered spikes for an example D1-MSN recorded from this mouse. Time 0 indicates the start of spout contact. Both the lick PETH and the lick-triggered spike PETH were smoothed with a Gaussian (σ = 25 ms).

(B) Upper, lick rasters and lick PETH computed using licks around ±200 ms of each lick for an example D2-Cre mouse. Lower, rasters and PETH of lick-triggered spikes for an example D2-MSN recorded from this mouse. Similar to that described in (A).

(C) Correlation between the lick PETH and the lick-triggered spike PETH in (A). Both PETHs were binned at 10 ms.

(D) Correlation between the lick PETH and the lick-triggered spike PETH in (B). Both PETHs were binned at 10 ms.

(E) Distribution of the phase corresponding to the peak of lick-triggered oscillatory activity for D1-MSNs (n = 66).

(F) Distribution of the phase corresponding to the peak of lick-triggered oscillatory

activity for D2-MSNs (n = 58).

(G) Population average (mean ± SEM) of z-scored lick-triggered spike PETH for D1-MSNs and D2-MSNs ($F_{interaction(35, 4270)} = 7.76$, $p < 1\times10^{-15}$, two-way ANOVA with mixed design).

See also Figure S4.

Figure 4. Transient Inactivation of D1-MSNs during Tongue Protrusion Reduces Lick Probability

(A) Example lick signals of laser-off and laser-on trials (5 trials for each) in a D1-Cre mouse in which AAV2/8-CAG-DIO-GtACR1-P2A-EGFP was bilaterally injected in VLS. The lick signals were aligned to the onset of the second lick. Green shading indicates the duration of laser stimulation. The lick signals were detected by the interruption of an infrared beam and were sign-reversed for display purpose.

(B) Transient inactivation of D1-MSNs around the time of tongue protrusion of the third lick event significantly reduced the amplitude of lick signal ($F_{(1, 6)} = 78.2$, $p = 1.16\times10^{-4}$, two-way repeated measures ANOVA). The lick signals were aligned to laser onset. Gray shading indicates the duration of laser stimulation. Black horizontal line marks the time points in which the amplitude of lick signal was significantly different between laser-off and laser-on conditions. Data represent mean ± SEM.

(C) Transient inactivation of D1-MSNs around the time of tongue protrusion significantly reduced the lick probability of the third lick event (left, p = 0.016,

Wilcoxon signed rank test) but not that of the next lick event (right, p = 0.58, n = 7 mice, Wilcoxon signed rank test).

(D) Transient inactivation of D1-MSNs around the time of tongue protrusion did not affect bout length (p = 0.58, n = 7 mice, Wilcoxon signed rank test).

(E) Example lick signals of laser-off and laser-on trials (5 trials for each) in a D2-Cre mouse in which AAV2/8-CAG-DIO-GtACR1-P2A-EGFP was bilaterally injected in VLS. Similar to that described in (A).

(F) Transient inactivation of D2-MSNs around the time of tongue protrusion of the third lick event did not change the amplitude of lick signal ($F_{(1, 5)}$ = 1.2, p = 0.32, two-way repeated measures ANOVA). Similar to that described in (B). Data represent mean ± SEM.

(G) Transient inactivation of D2-MSNs around the time of tongue protrusion did not change lick probability of the third lick event (p = 0.69, Wilcoxon signed rank test) or the fourth lick event (p = 0.44, n = 6 mice, Wilcoxon signed rank test).

(H) Transient inactivation of D2-MSNs around the time of tongue protrusion did not affect bout length (p = 1, n = 6 mice, Wilcoxon signed rank test).

See also Figure S5.

Figure 5. Role of Endogenous D1-MSNs Activity in Controlling SNr Responses during Licking Movement

(A) Left, schematic of recording from SNr while bilateral inactivation of D1-MSNs in VLS. Right, example fluorescence image showing the electrode track in SNr

marked by DiO.

(B) For D1-Cre mice used in electrophysiological recording of SNr neurons, inactivation of D1-MSNs in VLS significantly reduced the amplitude of lick PSTH ($F_{(1, 18)} = 44.46$, $p = 2.96\times10^{-6}$, two-way repeated measures ANOVA). Data represent mean ± SEM. Gray shading indicates the duration of laser stimulation.

(C) Left, the responses of SNr neurons (n = 13) that showed significant increase in firing rates after inactivation of D1-MSNs in VLS. For each neuron, the responses were normalized by the peak firing rate in laser-off condition. Data represent mean ± SEM. Gray shading indicates the duration of laser stimulation. Right, distribution of response types for those SNr neurons that significantly increased firing rate after inactivation of D1-MSNs in VLS.

(D) Left, the responses of SNr neurons (n = 40) that showed significant decrease in firing rates after inactivation of D1-MSNs in VLS. Similar to that described in (C). Right, distribution of response types for those SNr neurons that significantly decreased firing rate.

(E) Left, the responses of SNr neurons (n = 107) that did not significantly change firing rates after inactivation of D1-MSNs in VLS. Similar to that described in (C). Right, distribution of response types for those SNr neurons that did not significantly change firing rate.

(F) For D1-Cre mice used in electrophysiological recording of SNr neurons, transient inactivation of D1-MSNs in VLS around the time of tongue protrusion significantly reduced the amplitude of lick signal for the third lick event ($F_{(1, 11)} = 40.8$, $p =$

5.2×10^{-5}, two-way repeated measures ANOVA). The lick signals were aligned to laser onset. Data represent mean ± SEM. Gray shading indicates the duration of laser stimulation.

(G) Left, the responses of SNr neurons (n = 19) that showed significant rate increase within the time window of the third lick event after transient inactivation of D1-MSNs in VLS. For each neuron, the responses were normalized by the peak firing rate in laser-off condition. Data represent mean ± SEM. Gray shading indicates the duration of laser stimulation. Right, distribution of response types for those SNr neurons that significantly increased firing rate within the time window of the third lick event after transient inactivation of D1-MSNs in VLS.

(H) Left, the responses of SNr neurons (n = 14) that showed significant rate decrease within the time window of the third lick event after transient inactivation of D1-MSNs in VLS. Similar to that described in (G). Right, distribution of response types for those SNr neurons that significantly decreased firing rate within the time window of the third lick event.

(I) Left, the responses of SNr neurons (n = 79) that did not significantly change firing rate within the time window of the third lick event after transient inactivation of D1-MSNs in VLS. Similar to that described in (G). Right, distribution of response types for those SNr neurons that did not significantly change firing rate within the time window of the third lick event.

See also Figure S6.

Figure 6. Role of Endogenous D2-MSNs Activity in Controlling SNr Responses during Licking Movement

(A) Left, schematic of recording from SNr while bilateral inactivation of D2-MSNs in VLS. Right, example fluorescence image showing the electrode track in SNr marked by DiO.

(B) For D2-Cre mice used in electrophysiological recording of SNr neurons, inactivation of D2-MSNs in VLS significantly increased the amplitude of lick PSTH ($F_{(1, 16)} = 69.26$, $p = 3.31\times10^{-7}$, two-way repeated measures ANOVA). Data represent mean ± SEM. Gray shading indicates the duration of laser stimulation.

(C) Upper, the responses of SNr neurons (n = 8) that showed significant decrease in firing rates after inactivation of D2-MSNs in VLS. For each neuron, the responses were normalized by the peak firing rate in laser-off condition. Data represent mean ± SEM. Gray shading indicates the duration of laser stimulation. Lower, distribution of response types for those SNr neurons that significantly decreased firing rate after inactivation of D2-MSNs in VLS.

(D) Upper, the responses of SNr neurons (n = 22) that showed significant increase in firing rates after inactivation of D2-MSNs in VLS. Similar to that described in (C). Lower, distribution of response types for those SNr neurons that significantly increased firing rate.

(E) Upper, the responses of SNr neurons (n = 73) that did not significantly change firing rates after inactivation of D2-MSNs in VLS. Similar to that described in (C). Lower, distribution of response types for those SNr neurons that did not significantly

change firing rate.

See also Figure S6.

STAR*METHODS

RESOURCE AVAILABILITY

Lead Contact

Further information and requests for resources and reagents should be directed to and will be fulfilled by the Lead Contact, Haishan Yao (haishanyao@ion.ac.cn).

Materials Availability

This study did not generate new unique reagents.

Data and Code Availability

All data, custom scripts and functions used for this study are available from the Lead Contact, Haishan Yao (haishanyao@ion.ac.cn).

EXPERIMENTAL MODEL AND SUBJECT DETAILS

Animals

All animal procedures were approved by the Animal Care and Use Committee at the Institute of Neuroscience, Center for Excellence in Brain Science and Intelligence Technology, Chinese Academy of Sciences (IACUC No. NA-013-2019). We used the following mice: D1-Cre (Tg(Drd1a-cre)262Gsat/Mmcd), D2-Cre (Tg(Drd2-cre)ER44Gsat/Mmcd) (Gong et al., 2007) and C57BL/6 mice. Adult (2–4 months at the time of surgery) male mice were used for all experiments. All mice were housed on a

12 h:12 h light/dark cycle in the Institute of Neuroscience animal facility, with the humidity controlled at 40–70% and temperature at 22–23°C.

METHOD DETAILS

Adeno-Associated Virus

We used the following AAVs: AAV2/5-hSyn-hGtACR1-EGFP-WPRE (titer: 2–3×10^{12} viral particles/ml; for inactivation of VLS or DS); AAV2/8-CAG-DIO-GtACR1-P2A-EGFP (titer: 2–3×10^{12} viral particles/ml; for inactivation of D1-MSNs or D2-MSNs in VLS); AAV2/8-Syn-FLEX-ChrimsonR-tdTomato (titer: 2–3×10^{12} viral particles/ml; for optogenetic tagging of D1- or D2-MSNs); AAV2/8-hSyn-eGFP-3Flag-WPRE-SV40pA or AAV2/8-hSyn-FLEX-tdTomato (titer: 2–3×10^{12} viral particles/ml; for optogenetic experiments as a control group).

Surgery

Before surgery, the mice were anesthetized with a mixture of fentanyl (0.05 mg/kg), medetomidine (0.5 mg/kg) and midazolam (5 mg/kg) injected intraperitoneally, and were head-fixed in a stereotaxic apparatus. To target VLS or DS, two craniotomies (~ 0.5 mm diameter) were performed bilaterally above VLS (AP 0.34 mm, ML ±2.75 mm) or DS (AP 1.0 mm, ML ±1.8 mm). The virus was injected with a glass pipette (15–20 μm tip diameter) using a syringe pump (Harvard Apparatus). We injected 400–500 nl of AAV in VLS at a depth of 3.2 mm and in DS at a depth of 2.0 mm. After the virus injection, the pipette was left in place for 15–30 minutes before retraction. For mice

used in optogenetic inactivation experiments, optical fiber (200 μm diameter, NA 0.37) was inserted 200–300 μm above the injection site following the virus injection. A stainless-steel headplate was fixed to the skull using dental cement. For mice used in extracellular recording from VLS or SNr, the skull region above the recording site was marked with permanent ink. After the surgery, the mice were given Rimadyl via drinking water for 3 days, and were allowed to recover with food and water ad libitum for at least 10 days.

In some C57BL/6 mice (n = 6), fluorescently conjugated Cholera toxin subunit B (CTB-555, 2 μg/μl, 300 nl, Invitrogen) was injected unilaterally into VLS. The histology experiments were performed 2 weeks after the injection.

Behavioral task

Mice were deprived of water for 2 days before the behavioral training. During behavioral experiments, the mouse was head-fixed and sat in an acrylic tube. The lick spout was located around 5 mm in front of the tip of the nose and 0.5 mm below the lower lip. Touch of the spout by forelimbs was prevented by a block of plastic plate. Tongue licks were detected by an electrical lick sensor (Weijnen, 1989) or the interruption of an infrared beam if the mice were used for electrophysiological recordings. Fluid delivery was controlled by a peristaltic valve (Kamoer). An Arduino microcontroller platform was used for lick measurement, fluid delivery, and laser stimulation. A multifunction I/O device (USB-6001, National Instruments) was used for data acquisition. The lick signals and task-related signals were sampled at 2000 Hz.

For voluntary licking task, mice went through a habituation phase, a free-drinking phase, and a final task phase. During the habituation phase (2–3 days), the mouse was handled by the experimenter for 5–10 min and learned to lick water (300–500 nl) from a syringe. During the free-drinking phase (1–2 days), the mouse was head-fixed into the behavioral apparatus. Water (0.3–0.5 μl) was delivered every time a lick was detected. The mouse was head-fixed for at least 30 min, and the lick spout was removed after the mouse consumed 1000 μl of water. During the final task phase, sucrose (10% wt/vol) was used. The delivery of sucrose was triggered if a lick was preceded by at least 1 s of no licks (or 1.5 s of no licks for electrophysiological recordings of D1- and D2-MSNs), and the time window of lick-triggered delivery of sucrose lasted for 3 s for most experiments and lasted for 4 s for some experiments. For optogenetic inactivation experiments with 2 s of laser stimulation or for electrophysiological recording experiments, during the time window of sucrose delivery, 1 μl was delivered after the first lick and 0.3–0.5 μl was delivered after each of the following licks. For optogenetic inactivation experiments with 25 ms or 150 ms of laser stimulation, 0.5 μl of sucrose was delivered every 3 licks. After the time-window of sucrose delivery, there was a waiting period, in which a lick would not trigger the delivery of sucrose. The waiting period lasted for 2 s for the experiments of inactivating striatum (VLS or DS) and 1 s for those electrophysiological experiments in which D1- or D2-MSNs were recorded. Each mouse performed the task for 0.5 h in each session. After being trained in the final task phase for 2–3 days, the mice were used for optogenetic or electrophysiological experiments.

Optogenetic stimulation

Optical activation of GtACR1 (ChrimsonR) was induced by green (red) light. A green laser (520 or 532 nm) or a red laser (635 nm) (Shanghai Laser & Optics Century Co.) was connected to an output optical fiber and the laser stimulation was controlled by an Arduino microcontroller.

For optogenetic inactivation experiments, trials with and without laser stimulation were interleaved. For optogenetic stimulation with 2 s of laser, laser stimulation was triggered by the first lick of a lick bout that was preceded by at least 1 s of no licks. Laser was at a power of 8 or 10 mW at fiber tip.

For optogenetic stimulation with 25 ms of laser, the inter-lick interval of the mouse was first estimated from a few lick bouts, and laser stimulation was triggered after an inter-lick interval following the onset of the second lick in a lick bout. For optogenetic stimulation with 150 ms of laser, laser stimulation was triggered at 3 s following the onset of lick bout. Laser was at a power of 40 mW at fiber tip.

Optogenetic tagging

For optogenetic tagging of D1- and D2-MSNs, red laser light (1–3 mW at fiber tip) was applied to the fiber of the optrode. We delivered 100 trials of 100 ms laser stimulation, with a 5 s inter-trial interval (Lee et al., 2019). To identify a unit as ChrimsonR-expressing, we required that the unit was significantly activated by laser stimulation, the latency of laser-evoked spikes was < 6 ms and the Pearson's correlation coefficient

between waveforms (1.6 ms duration) of laser-evoked spikes and spontaneous spikes was > 0.95 (Lee et al., 2019). We used a paired t test to compare the spike number between the spikes in a 1-s period before laser onset and the spikes in a 6-ms period after laser onset, and those units with $p < 0.01$ were considered to be significantly activated by laser stimulation (Lee et al., 2019). These criteria yielded 111 identified ChrimsonR-expressing units in D1-Cre mice (out of 712 total units from 7 mice), 96 identified ChrimsonR-expressing units in D2-Cre mice (out of 784 total units from 6 mice) and 0 false positives (out of 275 total units from 2 control mice) (Figure S3B).

In vivo extracellular recording

Optogenetic tagging and recordings were performed at least 3 weeks after the virus injection. Before the recording, the mice were head-fixed to a holder attached to the stereotaxic apparatus and anesthetized with isoflurane (1–2%). A craniotomy (~ 1 mm diameter) was made above VLS (AP 0.34 mm, ML ±2.75 mm) or SNr (AP -3.3 to -3.8 mm; ML ±1.65 mm). The dura was removed, and the craniotomy was protected by a silicone elastomer (Kwik-Cast, WPI). The mouse was allowed to recover from the anesthesia in home cage for at least 2 hours. The recordings were made with optrodes (ASSY-37-32-1-9mm, Diagnostic Biochips) or multi-site silicon probes (A1×32-Poly2-10mm-50s-177-A32, NeuroNexus Technologies) mounted on a manipulator (MX7630/45DR, Siskiyou Corporation). The electrodes were coated with DiI or DiO (Invitrogen) to allow post hoc recovery of penetration track. After finishing the recordings, the electrode was retracted. The craniotomy was cleaned with saline and

covered with a silicone elastomer (Kwik-Cast, WPI). We made 1–4 sessions of recordings from each mouse.

The neural responses were amplified and filtered using a Cerebus 32-channel system (Blackrock microsystems). Spiking signals were sampled at 30 kHz. To detect the waveforms of spikes, we band-pass filtered the signals at 250–7500 Hz and set a threshold at 3.5 or 4 SD of the background noise. Spikes were sorted offline using the Offline Sorter (Plexon Inc.) based on cluster analysis of principle component amplitude. Spike clusters were considered to be single units if the interspike interval was larger than 1.5 ms and the p value for multivariate analysis of variance tests on clusters was less than 0.05. Task-related events were digitized as TTL levels and recorded by the Cerebus system.

Slice preparation and recording

We used D1-Cre and D2-Cre mice for slice recordings. Mice that had been injected with AAV2/8-CAG-DIO-GtACR1-P2A-EGFP in the VLS were anesthetized with isoflurane and perfused with ice-cold oxygenated (95% O_2/5% CO_2) solution containing the following (in mM): 2.5 KCl, 1.25 NaH_2PO_4, 2 Na_2HPO_4, 2 $MgSO_4$, 213 sucrose, 26 $NaHCO_3$. The mouse brain was dissected, and coronal slices including VLS (250 μm) were prepared using a vibratome (VT1200S, Leica) in the ice-cold oxygenated cutting solution. The prepared brain slices were incubated in artificial cerebral spinal fluid (ACSF), which contained the following (in mM): 126 NaCl, 2.5 KCl, 1.25 NaH_2PO_4, 1.25 Na_2HPO_4, 2 $MgSO_4$, 10 Glucose, 26 $NaHCO_3$, 2 $CaCl_2$, for

at least 60 min at 34°C, and then were recorded at ~33°C with a temperature controller (Warner, TC324B).

D1- or D2-MSNs were identified as EGFP-expressing neurons under fluorescent microscope and visualized by infrared differential interference contrast (BX51, Olympus). Whole-cell recordings in current-clamp mode were made with a Multiclamp 700B amplifier and a Digidata 1440A (Molecular Devices). The electrodes (3−5 MΩ) were filled with an internal solution containing the following (in mM): 135 K-gluconate, 4 KCl, 10 HEPES, 10 sodium phosphocreatine, 4 Mg-ATP, 0.3 Na_3-GTP and 0.5 biocytin; pH:7.2, 276 mOsm. The spikes of GtACR1-expressiong neurons were induced by holding the membrane potential at -50 ~ -40 mV with current injection. For optogenetic stimulation, blue light (473 nm, 2 s duration, 12 mW mm^{-2}) was delivered through a ×40 objective using an X-Cite LED light source (Lumen Dynamics). Data were low-pass filtered at 10 kHz and sampled at 10 kHz.

Histology

The mouse was deeply anesthetized with isoflurane and was perfused with 25 ml saline followed by 25 ml paraformaldehyde (PFA, 4%). Brains were removed, fixed in 4% PFA (4℃) overnight, and then transferred to 30% sucrose in phosphate-buffered saline (PBS) until equilibration. Brains were sectioned at 50 μm using a cryostat (Microm). To observe EGFP fluorescence for brain slices of D1-Cre or D2-Cre mice injected with AAV2/8-CAG-DIO-GtACR1-P2A-EGFP, slices were incubated with blocking buffer (20% BSA, 0.5% Triton X-100 in PBS) for 2 h at room temperature

and then with primary antibody (rabbit anti-GFP, 1:1000, Invitrogen, G10362) diluted in blocking buffer overnight at 4°C. Slices were rinsed with PBS and incubated with secondary antibody (donkey anti-rabbit Alexa Fluor 594, 1:1000, Invitrogen, A21207) diluted in blocking buffer for 2 h at room temperature. The sections were rinsed with PBS, mounted onto glass slides and coverslipped with DAPI Fluoromount-G (SouthernBiotech, 0100-20) or Vectashield (Vector, H-1000). Fluorescence images were taken with VS120 (Olympus). Images were analyzed with ImageJ (NIH, US). The atlas schematics in the figures of this study are modified from (Franklin and Paxinos, 2007).

QUANTIFICATION AND STATISTICAL ANALYSIS

Data analysis

Analyses were performed in MATLAB. For the licking behavior, we generated timestamps for the onset and offset of each lick event (0.5 ms resolution) according to the analog voltage signal. The lick duration was the time from the onset to the offset of each lick event (i.e., the time period the tongue contacted the spout). The inter-lick interval was the interval between the onsets of two consecutive licks. A lick bout was defined as a group of licks in which the first lick was preceded by at least 1 s of no licks, the inter-lick interval of the first three licks was ≥ 0.3 s, and the last lick was followed by ≥ 0.5 s of no licks. For voluntary licking task, we constructed peri-stimulus time histogram (PSTH) for the licking behavior by aligning the first lick of all lick bouts and averaging the licks (200 ms/bin) across bouts. The lick rate in the voluntary licking task

was computed using licks within 2 s after bout onset. For the experiments in which 25-ms laser stimulation was applied around the time of tongue protrusion for the third lick event, we analyzed lick probability for the third and the fourth lick event. For the time window of the third (fourth) lick, the onset time was computed as the median time of the third (fourth) lick in laser-off trials minus 50 ms, and the offset time was computed as the median time of the third (fourth) lick in laser-off trials plus 50 ms. Lick probability for the third (fourth) lick event was defined as the probability that a lick occurred within the time window of the third (fourth) lick event.

For the optogenetic tagging experiments, the identified ChrimsonR-expressing units were further classified into putative MSNs, fast-spiking interneurons (FSIs) and tonically active neurons (TANs) based on their spike waveforms, firing rates and coefficients of variation (CV) of inter-spike intervals (Shin et al., 2018). TANs were defined as those with CVs < 1. For non-TAN units, MSNs were defined as those in which peak width > 0.42 ms and peak-valley width > 0.36 ms; FSIs were defined as those in which peak width < 0.42 ms, peak-valley width < 0.36 ms and mean firing rate > 1.5 Hz. Only units classified as putative MSNs and mean firing rate > 0.5 Hz were included in the analysis.

For SNr neurons, we classified the units into GABAergic and non-GABAergic neurons based on their spike waveforms (Figure S6B) (Barter et al., 2015). GABAergic SNr neurons were defined as those with peak width < 0.36 ms. Only units classified as GABAergic SNr neurons and mean firing rate > 1.5 Hz were included in the analysis.

To examine whether the activities of VLS or SNr neurons are related to the

start/stop or execution of lick sequence (Jin and Costa, 2010; Jin et al., 2014), we analyzed the spikes for those lick bouts whose length were between 1 s and 4 s. A trial of lick bout was defined to include a baseline phase (from -1 to -0.5 s relative to bout onset), a start phase (from -0.5 to 0.25 s relative to bout onset), an execution phase (the duration of the lick bout), and a stop phase (from -0.25 to 0.5 s relative to bout offset). For both the start and the stop phases, we divided the responses in 30 bins. For the execution phase, as the bout duration varied across different lick bouts during a recording session, we normalized the bout duration by dividing each bout in an equal number of 60 bins (Sales-Carbonell et al., 2018). The binned responses were averaged across all trials to obtain a PSTH. To determine whether the PSTH exhibits significant lick-related activity, we defined an upper (lower) threshold at 3 SD above (below) the mean firing rate in baseline phase. If the firing rates in > 1/3 bins of the execution phase were above the upper threshold (or below the lower threshold), the neuron was classified as a sustained (or inhibited) cell. For those cells whose responses in the execution phase were not different from the baseline (i.e., neither sustained nor inhibited cells), we defined start (or stop) cells as those whose firing rates in > 1/3 bins of the start (or stop) phase were above the upper threshold or below the lower threshold, and boundary cells as those in which significant change in firing rate was observed for both the start and the stop phases. Those neurons with significant response in at least one of the three phases were considered to exhibit lick-related activity.

To examine whether the activity of VLS neurons shows oscillatory activity related to the lick cycle, we computed lick-triggered spike peri-event time histogram (PETH)

using spikes occurring around ±200 ms of each lick, and lick PETH using licks occurring around ±200 ms of each lick within a lick bout (excluding the first two licks and the last two licks in the bout) (Rossi et al., 2016). Both the lick-triggered spike PETH and the lick PETH were smoothed with a Gaussian (σ = 25 ms). To determine whether the lick-triggered spike PETH showed oscillatory activity, we computed two Pearson's correlation coefficients for each unit, one was between the lick PETH and the lick-triggered spike PETH, and the other was between the lick PETH and the lick-triggered spike PETH shifted by 40 ms (corresponding to a phase shift of the spike PETH by ~ 90°) (10 ms/bin for both lick PETH and lick-triggered spike PETH) (Figure S4). If one of the two coefficients was significant ($p < 0.05$), the unit was considered to exhibit significant oscillatory activity related to the lick cycle and was used to analyze the oscillatory phase. To determine the phase relationship between the oscillatory neural activity and the lick cycle, we identified the time at which the amplitude of lick-triggered spike PETH was maximum and transformed it to polar coordinate.

For the responses of SNr neurons with and without inactivation of D1-MSNs (or D2-MSNs) in VLS, we used Wilcoxon signed rank test to compare the firing rates within the first 2 s of lick bout between laser-off and laser-on trials, or compare the firing rates within the time window of the third lick between laser-off and laser-on trials. Those SNr neurons with $p < 0.05$ were considered to exhibit significant rate increase or rate decrease. Only lick-related SNr neurons were included in this analysis.

Statistics

The statistical analysis was performed using MATLAB or GraphPad Prism (GraphPad Software). Wilcoxon signed rank test, Wilcoxon rank sum test, circular Watson-Williams two-sample test (Berens, 2009), χ^2 test, one-way repeated measures ANOVA, two-way ANOVA with mixed design, or two-way repeated measures ANOVA followed by Sidak's multiple comparisons test was used to determine the significance of the effect. Correlation values were computed using Pearson's correlation. Unless otherwise stated, data were reported as SEM.

ACKNOWLEDGEMENTS

This work was supported by the Strategic Priority Research Program of Chinese Academy of Sciences (grant No. XDB32010200), Shanghai Municipal Science and Technology Major Project (grant No. 2018SHZDZX05) and the National Natural Science Foundation of China (31771151).

AUTHOR CONTRIBUTIONS

Z.C., Z-Y. Z. and H. Y. conceived and designed the project. Z.C. and Z-Y. Z. performed most of the experiments and data analysis. T. X. helped with behavioral experiments. W. Z. and X-H. X. performed slice recordings. Y. L. helped with virus injection experiments. H. Y. wrote the manuscript, with feedback from all authors.

DECLARATION OF INTERESTS

The authors declare no competing interests.

REFERENCES

Albin, R.L., Young, A.B., and Penney, J.B. (1989). The functional anatomy of basal ganglia disorders. Trends Neurosci. *12*, 366-375.

Aldridge, J.W., and Berridge, K.C. (1998). Coding of serial order by neostriatal neurons: a "natural action" approach to movement sequence. J. Neurosci. *18*, 2777-2787.

Bakhurin, K.I., Li, X., Friedman, A.D., Lusk, N.A., Watson, G.D., Kim, N., and Yin, H.H. (2020). Opponent regulation of action performance and timing by striatonigral and striatopallidal pathways. Elife *9*, e54831.

Bakhurin, K.I., Mac, V., Golshani, P., and Masmanidis, S.C. (2016). Temporal correlations among functionally specialized striatal neural ensembles in reward-conditioned mice. J. Neurophysiol. *115*, 1521-1532.

Barbera, G., Liang, B., Zhang, L., Gerfen, C.R., Culurciello, E., Chen, R., Li, Y., and Lin, D.T. (2016). Spatially Compact Neural Clusters in the Dorsal Striatum Encode Locomotion Relevant Information. Neuron *92*, 202-213.

Barter, J.W., Li, S., Sukharnikova, T., Rossi, M.A., Bartholomew, R.A., and Yin, H.H. (2015). Basal ganglia outputs map instantaneous position coordinates during behavior. J. Neurosci. *35*, 2703-2716.

Berens, P. (2009). CircStat: A MATLAB Toolbox for Circular Statistics. Journal of Statistical Software *31*, 1-21.

Brown, J., Pan, W.X., and Dudman, J.T. (2014). The inhibitory microcircuit of the substantia nigra provides feedback gain control of the basal ganglia output. Elife *3*, e02397.

Cui, G., Jun, S.B., Jin, X., Pham, M.D., Vogel, S.S., Lovinger, D.M., and Costa, R.M. (2013). Concurrent activation of striatal direct and indirect pathways during action initiation. Nature *494*, 238-242.

DeLong, M.R. (1990). Primate models of movement disorders of basal ganglia origin. Trends Neurosci. *13*, 281-285.

Deniau, J.M., Kitai, S.T., Donoghue, J.P., and Grofova, I. (1982). Neuronal interactions in the substantia nigra pars reticulata through axon collaterals of the projection neurons. An electrophysiological and morphological study. Exp. Brain Res. *47*, 105-113.

Deniau, J.M., Mailly, P., Maurice, N., and Charpier, S. (2007). The pars reticulata of the substantia nigra: a window to basal ganglia output. Prog. Brain Res. *160*, 151-172.

dos Santos, L.M., Boschen, S.L., Bortolanza, M., de Oliveira, W.F., Furigo, I.C., Mota-Ortiz, S.R., Da Cunha, C., and Canteras, N.S. (2012). The role of the ventrolateral caudoputamen in predatory hunting. Physiol. Behav. *105*, 893-898.

dos Santos, L.M., Ferro, M.M., Mota-Ortiz, S.R., Baldo, M.V., da Cunha, C., and Canteras, N.S. (2007). Effects of ventrolateral striatal inactivation on predatory hunting. Physiol. Behav. *90*, 669-673.

Fan, D., Rossi, M.A., and Yin, H.H. (2012). Mechanisms of action selection and timing in substantia nigra neurons. J. Neurosci. *32*, 5534-5548.

Franklin, K.B.J., and Paxinos, G. (2007). The mouse brain in stereotaxic coordinates,

3rd Edition (Amsterdam, Boston: Elsevier Academic Press).
Freeze, B.S., Kravitz, A.V., Hammack, N., Berke, J.D., and Kreitzer, A.C. (2013). Control of basal ganglia output by direct and indirect pathway projection neurons. J. Neurosci. *33*, 18531-18539.
Geddes, C.E., Li, H., and Jin, X. (2018). Optogenetic Editing Reveals the Hierarchical Organization of Learned Action Sequences. Cell *174*, 32-43 e15.
Gerfen, C.R., Engber, T.M., Mahan, L.C., Susel, Z., Chase, T.N., Monsma, F.J., Jr., and Sibley, D.R. (1990). D1 and D2 dopamine receptor-regulated gene expression of striatonigral and striatopallidal neurons. Science *250*, 1429-1432.
Gong, S., Doughty, M., Harbaugh, C.R., Cummins, A., Hatten, M.E., Heintz, N., and Gerfen, C.R. (2007). Targeting Cre recombinase to specific neuron populations with bacterial artificial chromosome constructs. J. Neurosci. *27*, 9817-9823.
Gulley, J.M., Kosobud, A.E., and Rebec, G.V. (2002). Behavior-related modulation of substantia nigra pars reticulata neurons in rats performing a conditioned reinforcement task. Neuroscience *111*, 337-349.
Hikosaka, O. (2007). Basal ganglia mechanisms of reward-oriented eye movement. Ann N Y Acad Sci *1104*, 229-249.
Hikosaka, O., Takikawa, Y., and Kawagoe, R. (2000). Role of the basal ganglia in the control of purposive saccadic eye movements. Physiol. Rev. *80*, 953-978.
Hintiryan, H., Foster, N.N., Bowman, I., Bay, M., Song, M.Y., Gou, L., Yamashita, S., Bienkowski, M.S., Zingg, B., Zhu, M., *et al.* (2016). The mouse cortico-striatal projectome. Nat. Neurosci. *19*, 1100-1114.
Hunnicutt, B.J., Jongbloets, B.C., Birdsong, W.T., Gertz, K.J., Zhong, H., and Mao, T. (2016). A comprehensive excitatory input map of the striatum reveals novel functional organization. Elife *5*, e19103.
Isomura, Y., Takekawa, T., Harukuni, R., Handa, T., Aizawa, H., Takada, M., and Fukai, T. (2013). Reward-modulated motor information in identified striatum neurons. J. Neurosci. *33*, 10209-10220.
Jin, X., and Costa, R.M. (2010). Start/stop signals emerge in nigrostriatal circuits during sequence learning. Nature *466*, 457-462.
Jin, X., and Costa, R.M. (2015). Shaping action sequences in basal ganglia circuits. Curr. Opin. Neurobiol. *33*, 188-196.
Jin, X., Tecuapetla, F., and Costa, R.M. (2014). Basal ganglia subcircuits distinctively encode the parsing and concatenation of action sequences. Nat. Neurosci. *17*, 423-430.
Klaus, A., Alves da Silva, J., and Costa, R.M. (2019). What, If, and When to Move: Basal Ganglia Circuits and Self-Paced Action Initiation. Annu. Rev. Neurosci. *42*, 459-483.
Kravitz, A.V., Freeze, B.S., Parker, P.R., Kay, K., Thwin, M.T., Deisseroth, K., and Kreitzer, A.C. (2010). Regulation of parkinsonian motor behaviours by optogenetic control of basal ganglia circuitry. Nature *466*, 622-626.
Kravitz, A.V., Tye, L.D., and Kreitzer, A.C. (2012). Distinct roles for direct and indirect pathway striatal neurons in reinforcement. Nat. Neurosci. *15*, 816-818.
Lee, J., Wang, W., and Sabatini, B.L. (2020). Anatomically segregated basal ganglia

pathways allow parallel behavioral modulation. Nat. Neurosci. *23*, 1388-1398.
Lee, K., Bakhurin, K.I., Claar, L.D., Holley, S.M., Chong, N.C., Cepeda, C., Levine, M.S., and Masmanidis, S.C. (2019). Gain Modulation by Corticostriatal and Thalamostriatal Input Signals during Reward-Conditioned Behavior. Cell Rep *29*, 2438-2449 e2434.
Liu, D., Li, W., Ma, C., Zheng, W., Yao, Y., Tso, C.F., Zhong, P., Chen, X., Song, J.H., Choi, W.*, et al.* (2020). A common hub for sleep and motor control in the substantia nigra. Science *367*, 440-445.
London, T.D., Licholai, J.A., Szczot, I., Ali, M.A., LeBlanc, K.H., Fobbs, W.C., and Kravitz, A.V. (2018). Coordinated Ramping of Dorsal Striatal Pathways preceding Food Approach and Consumption. J. Neurosci. *38*, 3547-3558.
Markowitz, J.E., Gillis, W.F., Beron, C.C., Neufeld, S.Q., Robertson, K., Bhagat, N.D., Peterson, R.E., Peterson, E., Hyun, M., Linderman, S.W.*, et al.* (2018). The Striatum Organizes 3D Behavior via Moment-to-Moment Action Selection. Cell *174*, 44-58 e17.
Martiros, N., Burgess, A.A., and Graybiel, A.M. (2018). Inversely Active Striatal Projection Neurons and Interneurons Selectively Delimit Useful Behavioral Sequences. Curr. Biol. *28*, 560-573 e565.
Meng, C., Zhou, J., Papaneri, A., Peddada, T., Xu, K., and Cui, G. (2018). Spectrally Resolved Fiber Photometry for Multi-component Analysis of Brain Circuits. Neuron *98*, 707-717 e704.
Mink, J.W. (1996). The basal ganglia: focused selection and inhibition of competing motor programs. Prog. Neurobiol. *50*, 381-425.
Mittler, T., Cho, J., Peoples, L.L., and West, M.O. (1994). Representation of the body in the lateral striatum of the freely moving rat: single neurons related to licking. Exp. Brain Res. *98*, 163-167.
Moore, J.D., Kleinfeld, D., and Wang, F. (2014). How the brainstem controls orofacial behaviors comprised of rhythmic actions. Trends Neurosci. *37*, 370-380.
Nelson, A.B., and Kreitzer, A.C. (2014). Reassessing models of basal ganglia function and dysfunction. Annu. Rev. Neurosci. *37*, 117-135.
O'Hare, J.K., Ade, K.K., Sukharnikova, T., Van Hooser, S.D., Palmeri, M.L., Yin, H.H., and Calakos, N. (2016). Pathway-Specific Striatal Substrates for Habitual Behavior. Neuron *89*, 472-479.
Oldenburg, I.A., and Sabatini, B.L. (2015). Antagonistic but Not Symmetric Regulation of Primary Motor Cortex by Basal Ganglia Direct and Indirect Pathways. Neuron *86*, 1174-1181.
Park, J., Coddington, L.T., and Dudman, J.T. (2020). Basal Ganglia Circuits for Action Specification. Annu. Rev. Neurosci. *43*, 485-507.
Parker, J.G., Marshall, J.D., Ahanonu, B., Wu, Y.W., Kim, T.H., Grewe, B.F., Zhang, Y., Li, J.Z., Ding, J.B., Ehlers, M.D., and Schnitzer, M.J. (2018). Diametric neural ensemble dynamics in parkinsonian and dyskinetic states. Nature *557*, 177-182.
Pisa, M. (1988). Motor functions of the striatum in the rat: critical role of the lateral region in tongue and forelimb reaching. Neuroscience *24*, 453-463.
Pisa, M., and Schranz, J.A. (1988). Dissociable motor roles of the rat's striatum conform

to a somatotopic model. Behav. Neurosci. *102*, 429-440.

Redgrave, P., Prescott, T.J., and Gurney, K. (1999). The basal ganglia: a vertebrate solution to the selection problem? Neuroscience *89*, 1009-1023.

Rossi, M.A., Li, H.E., Lu, D., Kim, I.H., Bartholomew, R.A., Gaidis, E., Barter, J.W., Kim, N., Cai, M.T., Soderling, S.H., and Yin, H.H. (2016). A GABAergic nigrotectal pathway for coordination of drinking behavior. Nat. Neurosci. *19*, 742-748.

Rossi, M.A., and Yin, H.H. (2015). Elevated dopamine alters consummatory pattern generation and increases behavioral variability during learning. Front Integr Neurosci *9*, 37.

Sales-Carbonell, C., Taouali, W., Khalki, L., Pasquet, M.O., Petit, L.F., Moreau, T., Rueda-Orozco, P.E., and Robbe, D. (2018). No Discrete Start/Stop Signals in the Dorsal Striatum of Mice Performing a Learned Action. Curr. Biol. *28*, 3044-3055 e3045.

Schmidt, R., Leventhal, D.K., Mallet, N., Chen, F., and Berke, J.D. (2013). Canceling actions involves a race between basal ganglia pathways. Nat. Neurosci. *16*, 1118-1124.

Shin, J.H., Kim, D., and Jung, M.W. (2018). Differential coding of reward and movement information in the dorsomedial striatal direct and indirect pathways. Nat. Commun. *9*, 404.

Sippy, T., Lapray, D., Crochet, S., and Petersen, C.C. (2015). Cell-Type-Specific Sensorimotor Processing in Striatal Projection Neurons during Goal-Directed Behavior. Neuron *88*, 298-305.

Smith, Y., Bevan, M.D., Shink, E., and Bolam, J.P. (1998). Microcircuitry of the direct and indirect pathways of the basal ganglia. Neuroscience *86*, 353-387.

Taverna, S., Ilijic, E., and Surmeier, D.J. (2008). Recurrent collateral connections of striatal medium spiny neurons are disrupted in models of Parkinson's disease. J. Neurosci. *28*, 5504-5512.

Tecuapetla, F., Jin, X., Lima, S.Q., and Costa, R.M. (2016). Complementary Contributions of Striatal Projection Pathways to Action Initiation and Execution. Cell *166*, 703-715.

Tecuapetla, F., Matias, S., Dugue, G.P., Mainen, Z.F., and Costa, R.M. (2014). Balanced activity in basal ganglia projection pathways is critical for contraversive movements. Nat. Commun. *5*, 4315.

Toda, K., Lusk, N.A., Watson, G.D.R., Kim, N., Lu, D., Li, H.E., Meck, W.H., and Yin, H.H. (2017). Nigrotectal Stimulation Stops Interval Timing in Mice. Curr. Biol. *27*, 3763-3770 e3763.

Travers, J.B., Dinardo, L.A., and Karimnamazi, H. (1997). Motor and premotor mechanisms of licking. Neurosci Biobehav Rev *21*, 631-647.

Vandaele, Y., Mahajan, N.R., Ottenheimer, D.J., Richard, J.M., Mysore, S.P., and Janak, P.H. (2019). Distinct recruitment of dorsomedial and dorsolateral striatum erodes with extended training. Elife *8*, e49536.

von Krosigk, M., Smith, Y., Bolam, J.P., and Smith, A.D. (1992). Synaptic organization of GABAergic inputs from the striatum and the globus pallidus onto neurons in the substantia nigra and retrorubral field which project to the medullary reticular formation. Neuroscience *50*, 531-549.

Weijnen, J.A. (1989). Lick sensors as tools in behavioral and neuroscience research. Physiol. Behav. *46*, 923-928.

Weijnen, J.A. (1998). Licking behavior in the rat: measurement and situational control of licking frequency. Neurosci Biobehav Rev *22*, 751-760.

Xiao, X., Deng, H., Furlan, A., Yang, T., Zhang, X., Hwang, G.R., Tucciarone, J., Wu, P., He, M., Palaniswamy, R.*, et al.* (2020). A Genetically Defined Compartmentalized Striatal Direct Pathway for Negative Reinforcement. Cell *183*, 211-227 e220.

Figure 1

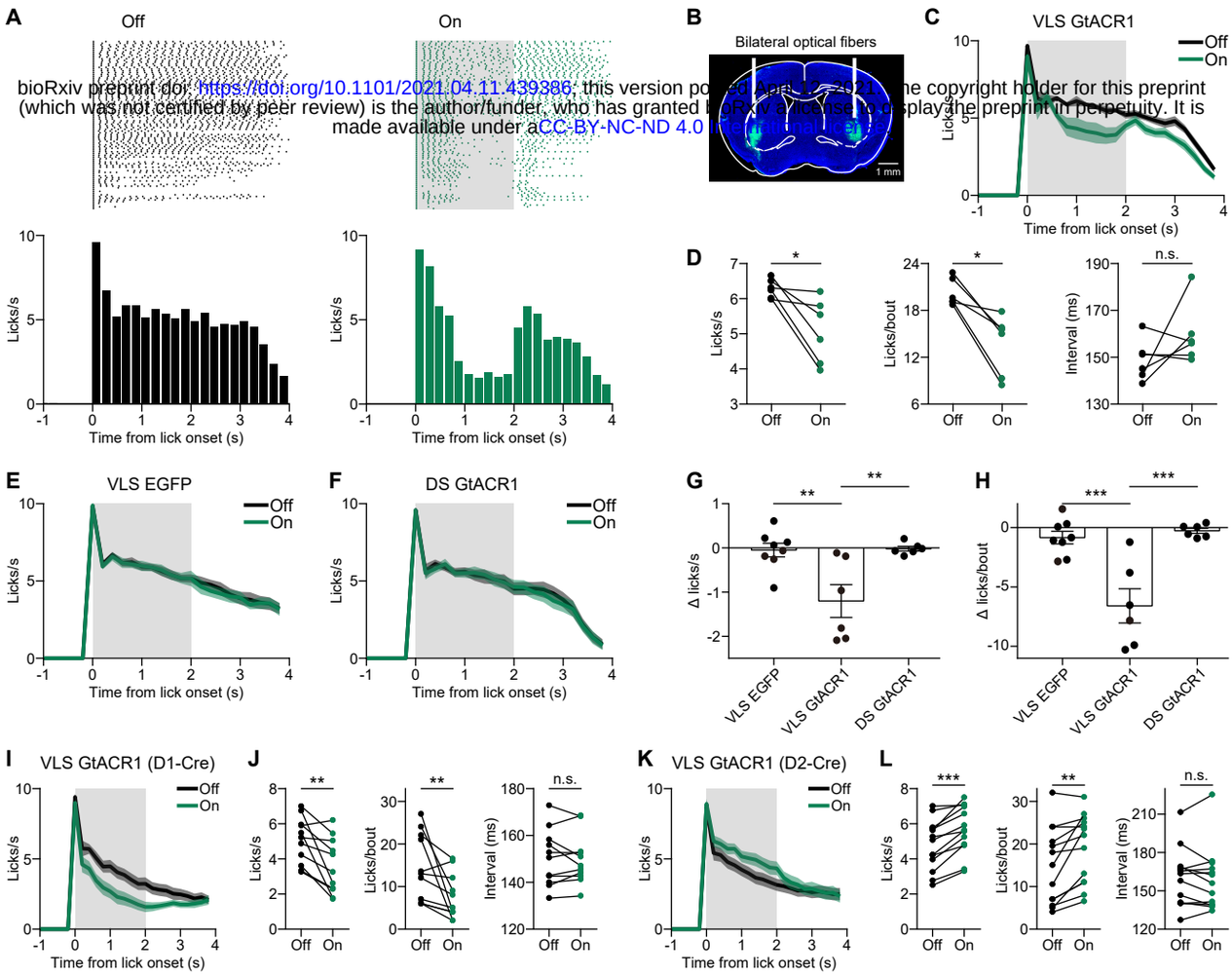

Figure 2

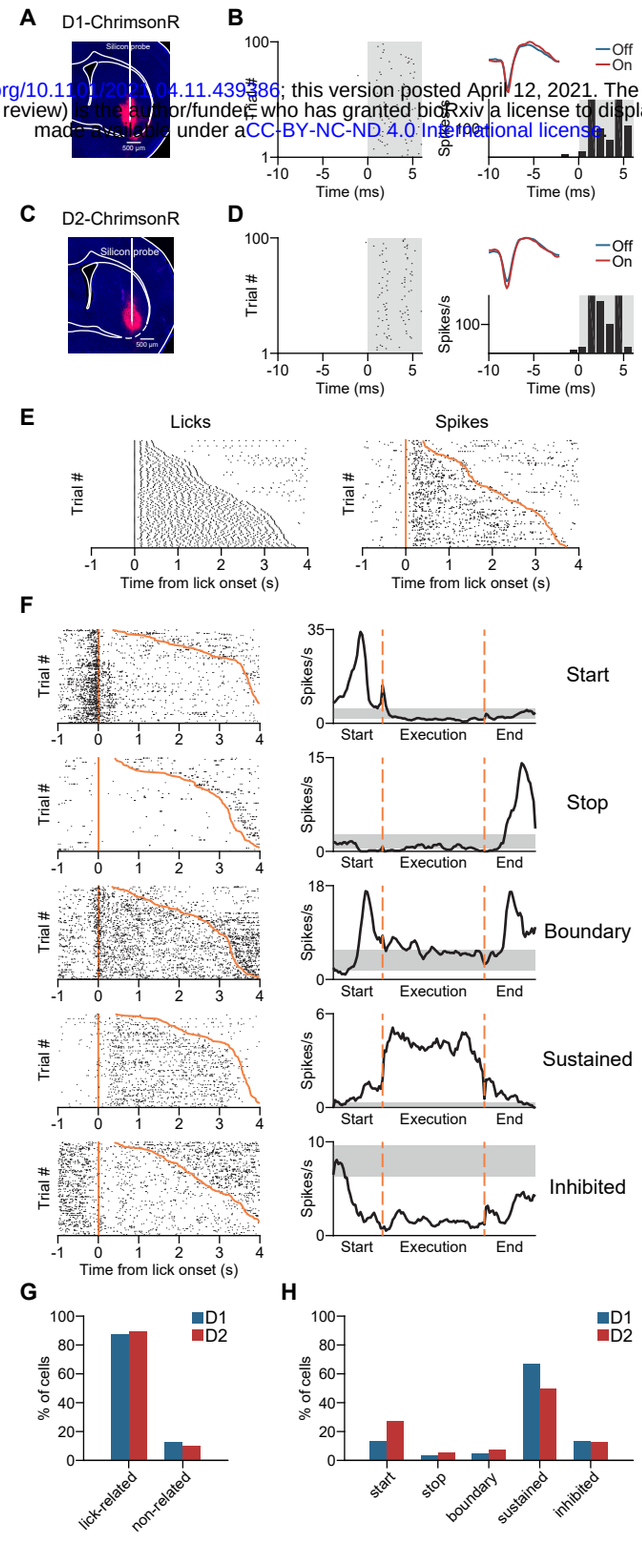

Figure 3

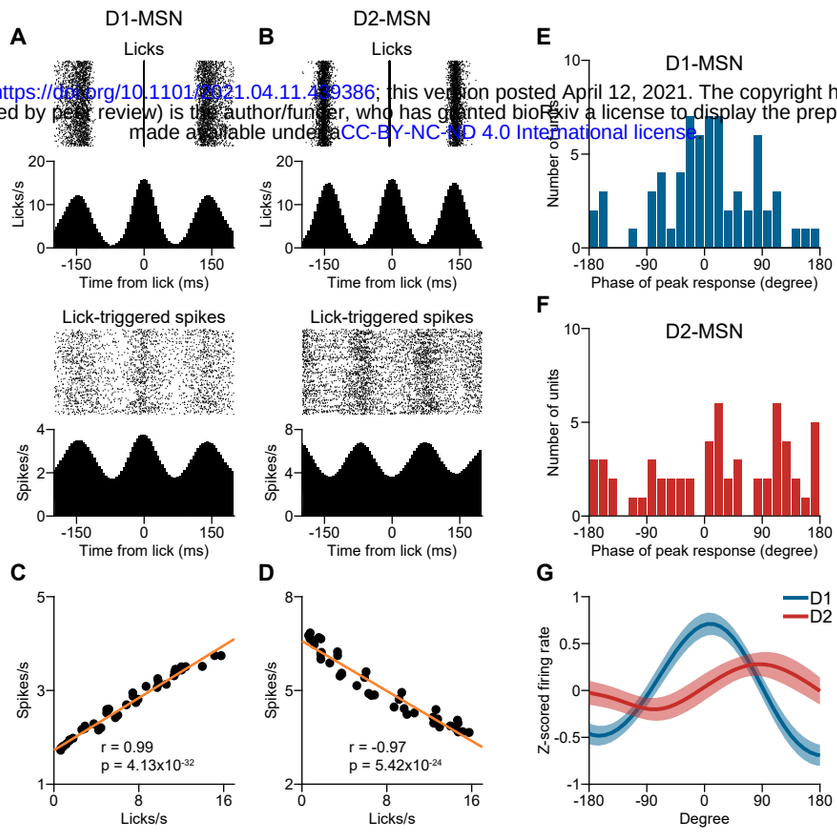

Figure 4

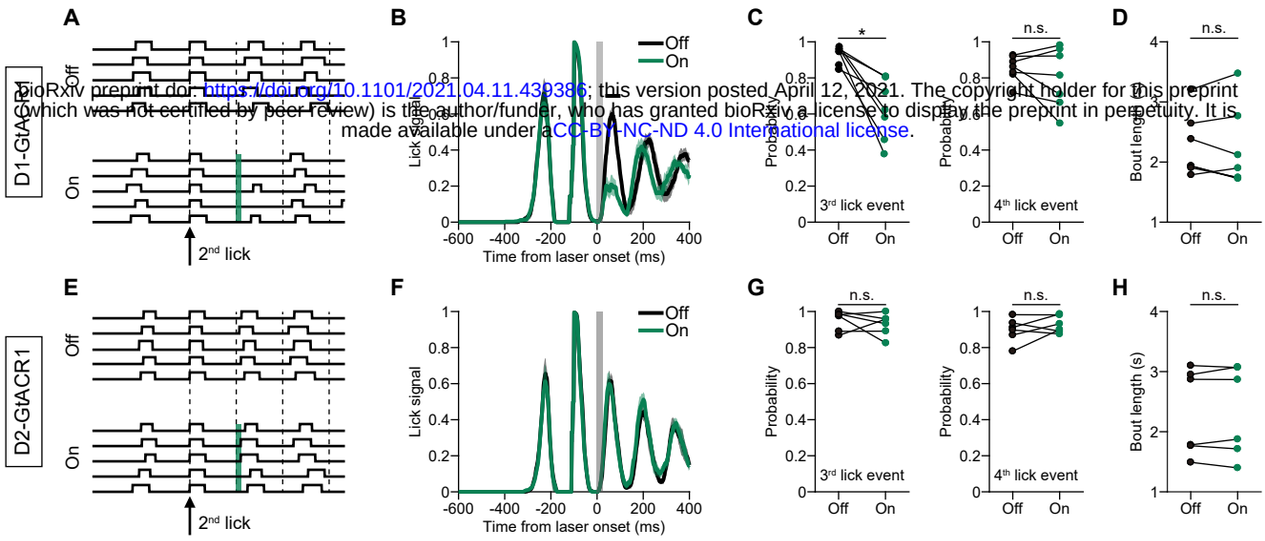

Figure 5

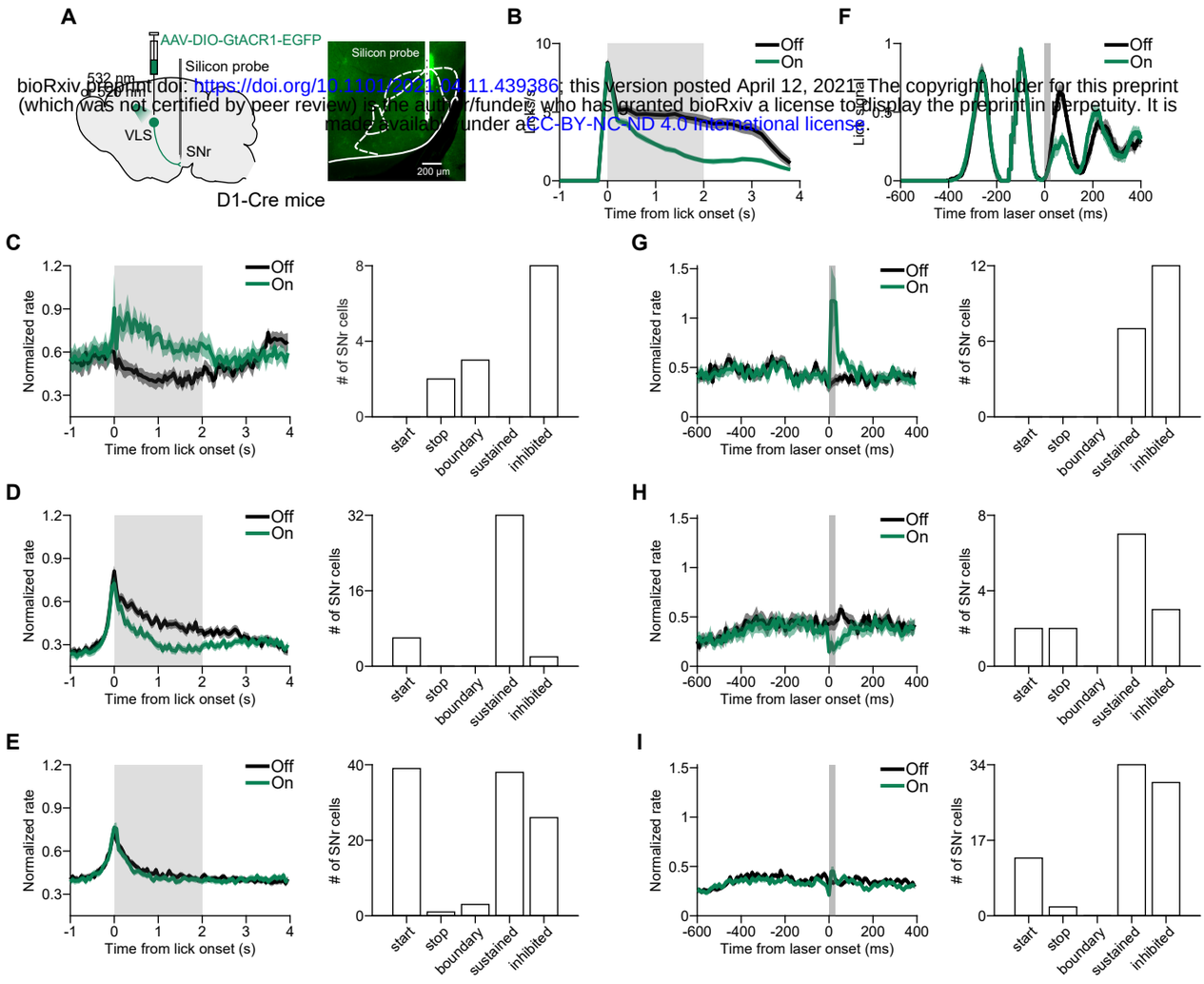

Figure 6

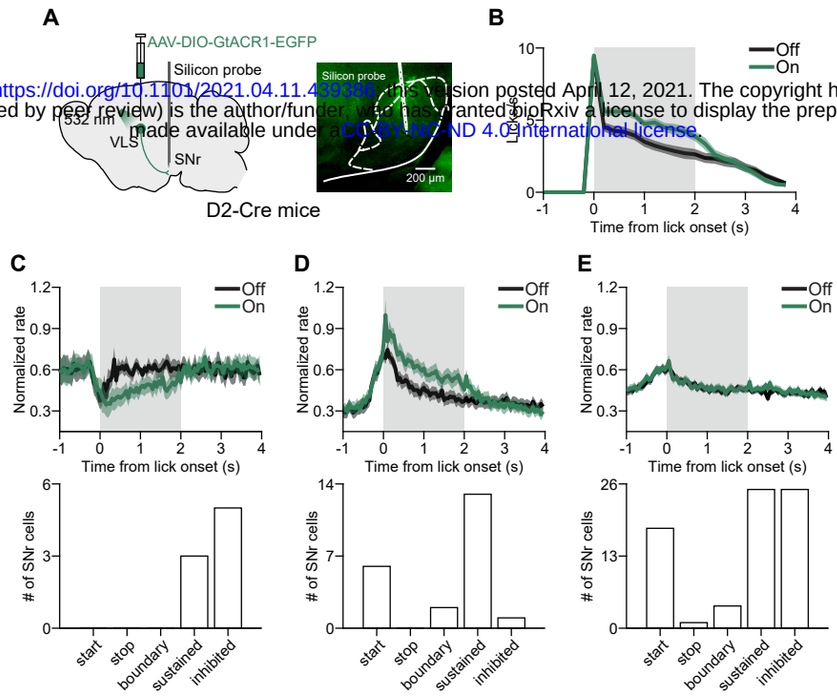

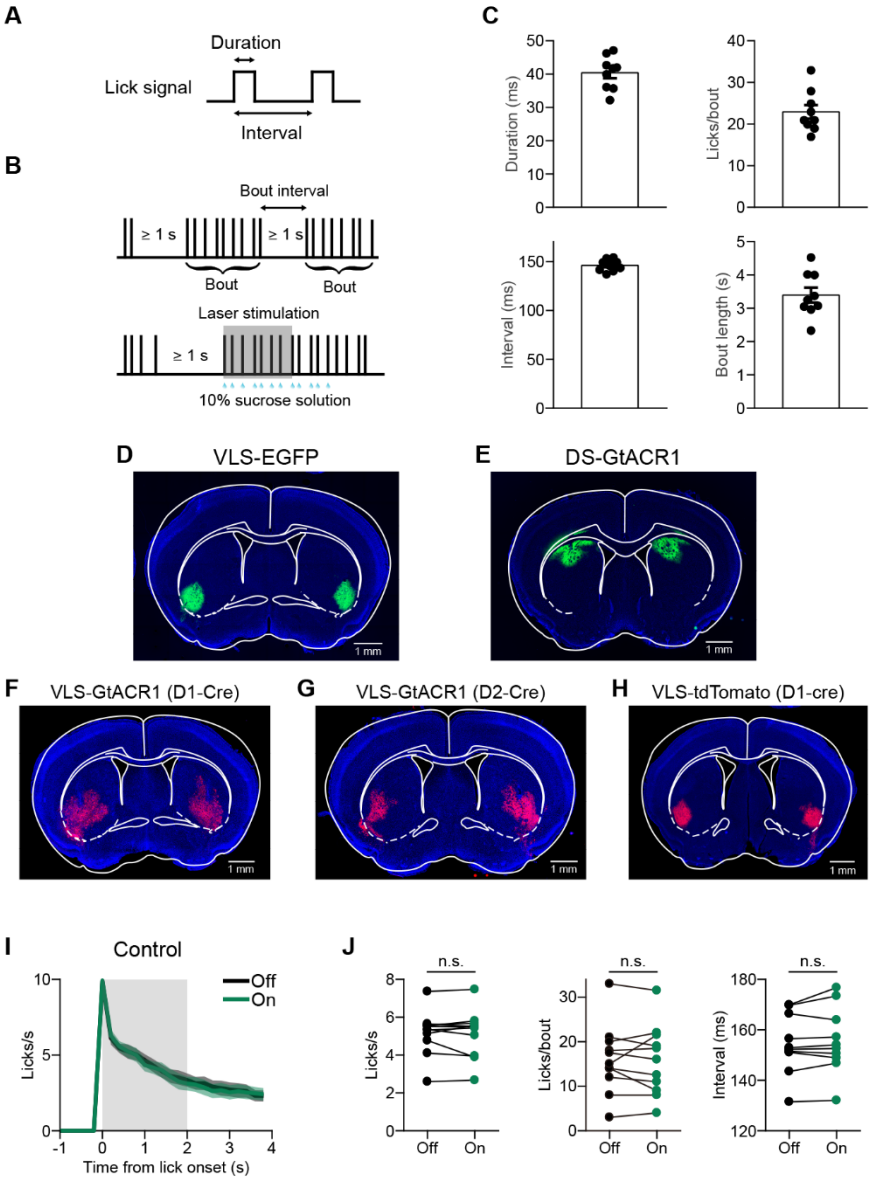

Figure S1. Parameters of Licking Behavior, Fluorescence Images of Virus Injection Sites and Effect of Laser Stimulation in Control Mice. Related to Figure 1.

(A) Measurement of lick duration and inter-lick interval from the lick signal.

(B) Definition of a valid lick bout and illustration of laser stimulation (gray shading), which was triggered by the first lick of a lick bout that was preceded by ≥ 1 s of no licks.

(C) Lick duration, inter-lick interval, number of licks per bout and bout length for the licking behavior of C57BL/6 mice (n = 9). Data represent mean ± SEM. For these mice, the time window of lick-triggered delivery of sucrose lasted for 4 s.

(D) Representative fluorescence image showing the expression of AAV2/8-hSyn-eGFP-3Flag-WPRE-SV40pA in VLS of a C57BL/6 mouse.

(E) Representative fluorescence image showing the expression of AAV2/5-hSyn-hGtACR1-EGFP-WPRE in DS of a C57BL/6 mouse.

(F and G) Representative fluorescence images showing the expression of AAV2/8-CAG-DIO-GtACR1-P2A-EGFP in VLS of a D1-Cre and a D2-Cre mouse. The EGFP

was observed using immunohistochemistry.

(H) Representative fluorescence image showing the expression of AAV2/8-hSyn-FLEX-tdTomato in VLS of a D1-Cre mouse.

(I) Laser stimulation in control D1-Cre mice (n = 5) and control D2-Cre mice (n = 6), in which AAV2/8-hSyn-FLEX-tdTomato was bilaterally injected in VLS, did not change the lick PSTH ($F_{(1, 10)}$ = 0.13, p = 0.72, two-way repeated measures ANOVA). Data represent mean ± SEM. Gray shading indicates the duration of laser stimulation.

(J) Laser stimulation in control D1-Cre mice (n = 5) and control D2-Cre mice (n = 6), in which AAV2/8-hSyn-FLEX-tdTomato was bilaterally injected in VLS, did not change lick rate (p = 0.97), number of licks per bout (p = 0.55) or inter-lick interval (p = 0.24, Wilcoxon signed rank test).

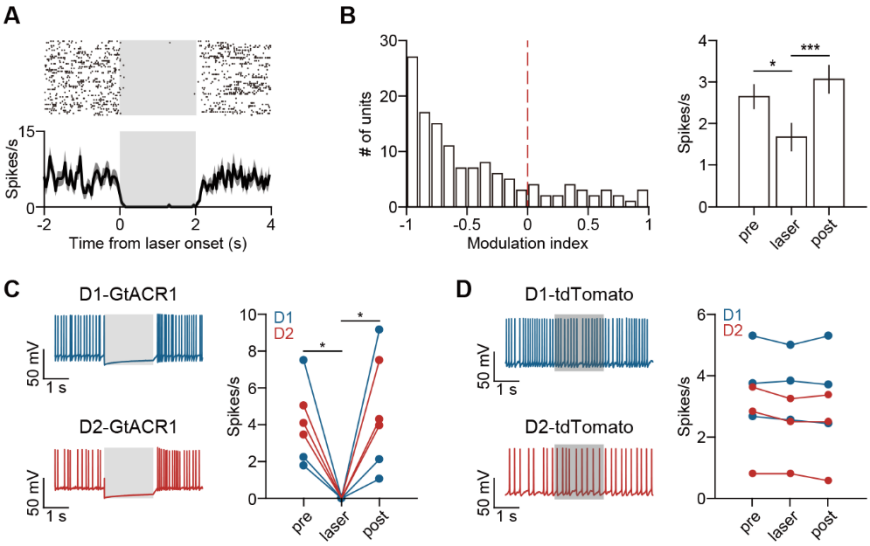

Figure S2. Activation of GtACR1 Suppresses Neuronal Activity in Vivo and in Slices. Related to Figure 1.

(A) Spike raster and PSTH for an example VLS neuron recorded from an awake C57BL/6 mouse, in which AAV2/5-hSyn-hGtACR1-EGFP-WPRE was expressed in VLS. Gray shading indicates the duration of laser stimulation.

(B) For C57BL/6 mice in which AAV2/5-hSyn-hGtACR1-EGFP-WPRE was expressed in VLS, laser stimulation significantly suppressed the firing of VLS neurons. Left, distribution of modulation index, defined as $(R_{laser} - R_{pre})/(R_{laser} + R_{pre})$, in which R_{laser} and R_{pre} are firing rates within a 2-s period during and before laser stimulation, respectively. $p = 2.35\times10^{-13}$, Wilcoxon signed rank test. Right, firing rates before, during and after laser stimulation. * $p < 0.05$, *** $p < 0.001$, one-way repeated measures ANOVA followed by Sidak's multiple comparisons test. n = 132 neurons from 2 mice. Data represent mean ± SEM.

(C) Left, responses of example D1-MSN and D2-MSN recorded from slices of D1-Cre and D2-Cre mice, in which AAV2/8-CAG-DIO-GtACR1-P2A-EGFP was injected in VLS. Gray shading indicates the duration of laser stimulation. Right, action potentials of D1- and D2-MSNs within a 2-s period before, during and after laser stimulation. * $p < 0.05$, one-way repeated measures ANOVA followed by Sidak's multiple comparisons test. n = 6 cells (3 D1-MSNs and 3 D2-MSNs).

(D) Left, responses of example D1- and D2-MSNs recorded from slices of D1-Cre or D2-Cre mice, in which AAV2/8-hSyn-FLEX-tdTomato was injected in VLS. Gray shading indicates the duration of laser stimulation. Right, the action potentials of D1- or D2-MSNs, which were induced by current injection, were not significantly affected by laser stimulation. $p > 0.05$, one-way repeated measures ANOVA. n = 6 cells (3 D1-MSNs and 3 D2-MSNs).

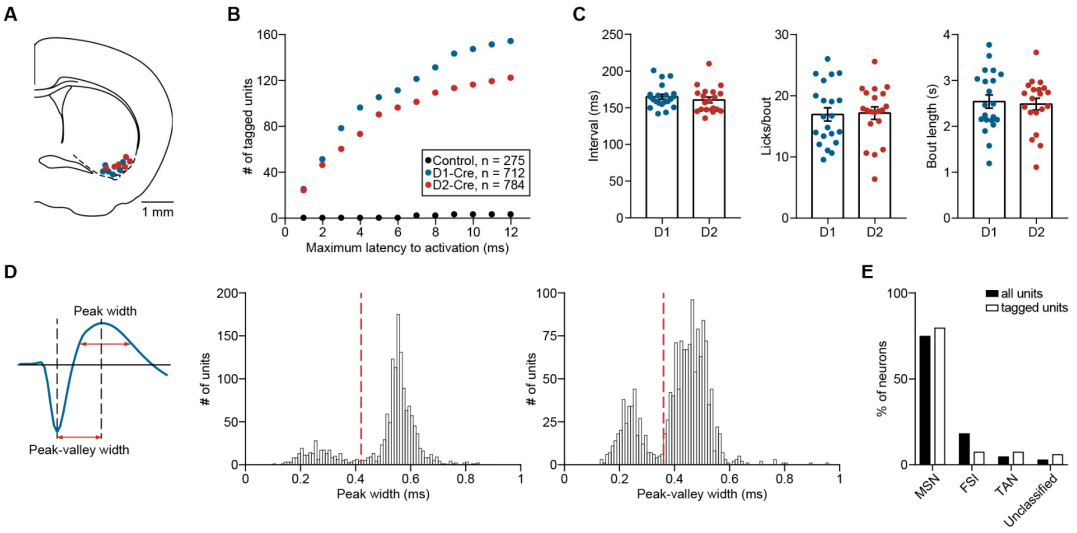

Figure S3. Spike Waveform Parameters of Units Identified by Optogenetic Tagging from the VLS of D1-Cre and D2-Cre Mice. Related to Figure 2.

(A) Each dot represents the location of the electrode tip in the last recording session for each mouse. Blue, sites of electrode tip for D1-Cre mice. Red, sites of electrode tip for D2-Cre mice. The distance between the uppermost and the lowermost recording sites in the electrode was 300 μm.

(B) Cumulative number of units identified by optogenetic tagging as a function of maximum latency to activation. Total number of cells for D1-Cre, D2-Cre and C57BL/6 mice were 712, 784, and 275, respectively.

(C) Licking parameters were not significantly different between D1-Cre and D2-Cre mice used in the optogenetic tagging experiments. Inter-lick interval: $p = 0.43$; number of licks per bout: $p = 0.72$; bout length: $p = 0.84$, Wilcoxon rank sum test. D1: n = 21 sessions from 6 D1-Cre mice; D2: n = 20 sessions from 6 D2-Cre mice. Data represent mean ± SEM.

(D) Left, illustration of the spike waveform parameters. Middle, Distribution of peak width for all units (n = 1496) recorded in the optogenetic tagging experiments. Right, Distribution of peak-valley width for all recorded units (n = 1496). For non-TAN units, MSNs were defined as those in which peak width > 0.42 ms (vertical dashed line in the middle panel) and peak-valley width > 0.36 ms (vertical dashed line in the right panel).

(E) Proportion of MSNs, FSIs, TANs and unclassified units among all recorded units (n = 1496) and tagged units (n = 207).

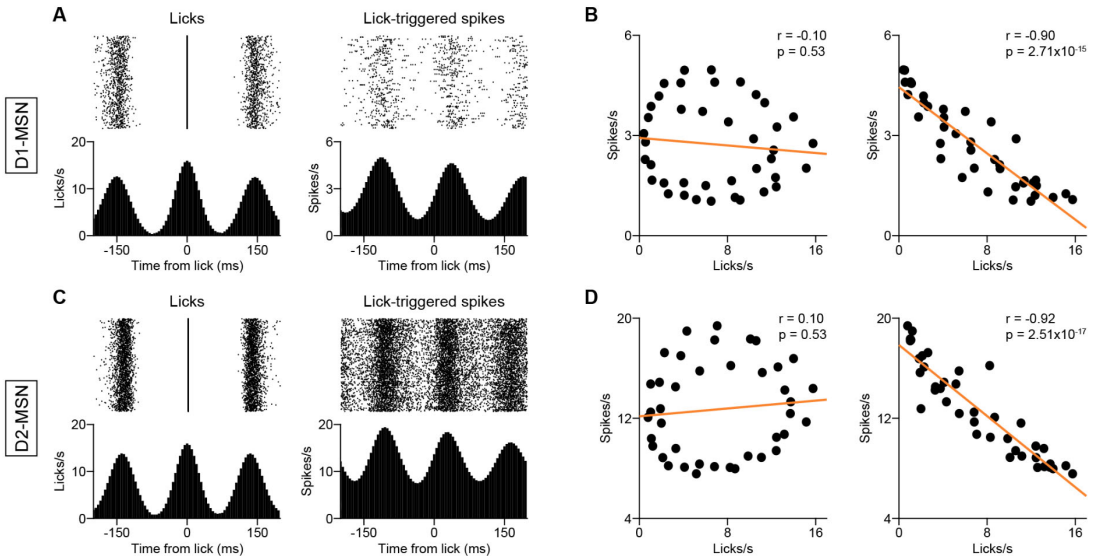

Figure S4. Correlation between Lick PETH and Lick-triggered Spike PETH. Related to Figure 3.

(A) Left, lick rasters and lick PETH computed using licks around ±200 ms of each lick, for an example D1-Cre mouse. Right, lick-triggered spikes (rasters and PETH), computed using spikes occurring around ±200 ms of each lick, for an example D1-MSN recorded from the mouse shown in the left. Both the lick PETH and the lick-triggered spike PETH were smoothed with a Gaussian (σ = 25 ms).

(B) Left, correlation between lick PETH and lick-triggered spike PETH in (A). Right, correlation between lick PETH in (A) and lick-triggered spike PETH in (A) shifted by 40 ms (corresponding to a phase shift of ~90^{o}). As one of the two coefficients was significant ($p < 0.05$), this unit was considered to exhibit significant oscillatory activity related to the lick cycle.

(C) Left, lick rasters and lick PETH computed using licks around ±200 ms of each lick, for an example D2-Cre mouse. Right, lick-triggered spikes (rasters and spike PETH), computed using spikes occurring around ±200 ms of each lick, for an example D2-MSN from the mouse shown in the left. Similar to that described in (A).

(D) Left, correlation between lick PETH and lick-triggered spike PETH in (C). Right, correlation between lick PETH in (C) and lick-triggered spike PETH in (C) shifted by 40 ms (corresponding to a phase shift of ~90^{o}). Similar to that described in (B).

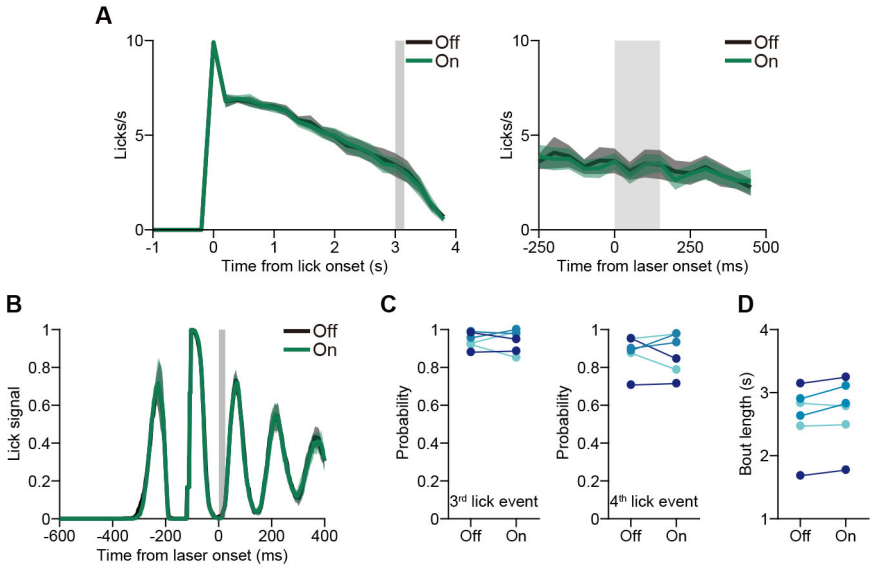

Figure S5. Effect of Transient Laser Stimulation on Licking for D2-GtACR1 Mice and Control Mice. Related to Figure 4.

(A) Inactivating D2-MSNs for 150 ms at 3 s after bout onset, when lick rate was lower, did not affect licking behavior. $F_{(1, 6)}$ = 0.18, p = 0.69, two-way repeated measures ANOVA. Data represent mean ± SEM. Gray shading indicates the duration of laser stimulation.

(B) Transient laser stimulation did not change the amplitude of lick signal for control D1-Cre mice in which AAV2/8-hSyn-FLEX-tdTomato was injected. $F_{(1, 5)}$ = 0.69, p = 0.45, two-way repeated measures ANOVA. Data represent mean ± SEM. The lick signals were aligned to laser onset. Gray shading indicates the duration of laser stimulation.

(C) Transient laser stimulation did not change the lick probability for control D1-Cre mice in which AAV2/8-hSyn-FLEX-tdTomato was injected. Left, for the third lick event, p = 1, Wilcoxon signed rank test. Right, for the fourth lick event, p = 1, Wilcoxon signed rank test. n = 6 sessions from 3 mice (each color represents one mouse).

(D) Transient laser stimulation did not change bout length for control D1-Cre mice in which AAV2/8-hSyn-FLEX-tdTomato was injected. p = 0.094, Wilcoxon signed rank test. n = 6 sessions from 3 mice (each color represents one mouse).

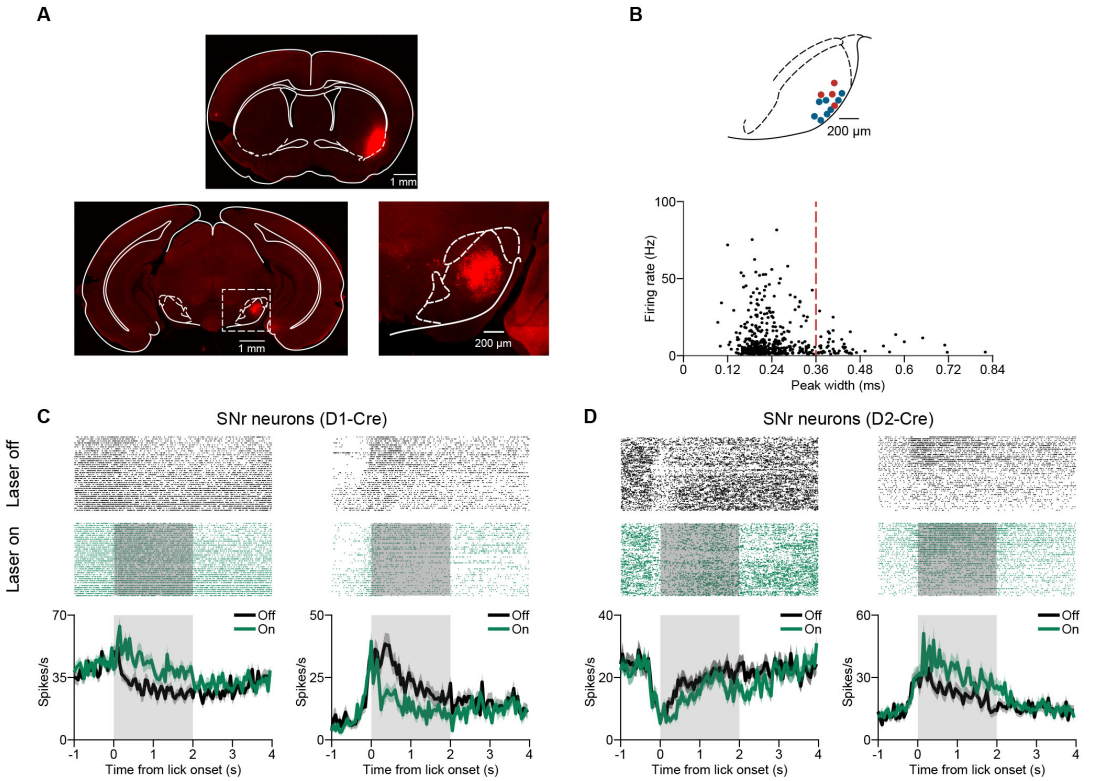

Figure S6. Recording from SNr while Inactivation of D1- or D2-MSNs in VLS. Related to Figure 5 and Figure 6.

(A) CTB-555 was injected in VLS (upper) and axon terminals from VLS were found in lateral part of SNr (lower). Lower right, enlarged view of image in the white box.

(B) Upper, each dot represents the location of electrode tip in the last recording session for each mouse. Blue, sites of electrode tip for D1-Cre mice. Red, sites of electrode tip for D2-Cre mice. The distance between the uppermost and the lowermost recording sites in the electrode was 775 μm. Lower, firing rate versus peak width of the SNr neurons (n = 512). Units with peak width < 0.36 ms were considered as GABAergic neurons.

(C) Inactivation of D1-MSNs in VLS caused an increase in firing rate in an example SNr neuron (left) and a decrease in firing rate in another example SNr neuron (right). Data represent mean ± SEM. Gray shading indicates duration of laser stimulation.

(D) Inactivation of D2-MSNs in VLS caused a decrease in firing rate in an example SNr neuron (left) and an increase in firing rate in another example SNr neuron (right). Data represent mean ± SEM. Gray shading indicates duration of laser stimulation.